Journal of Environmental Management 370 (2024) 122541

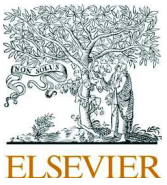

Contents lists available at ScienceDirect

Journal of Environmental Management

journal homepage: www.elsevier.com/locate/jenvman

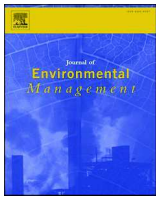

Research article

Multiscale morphological trajectories to support management of free-flowing rivers: the Vjosa in South-East Europe

Marta Crivellaro [a,*], Livia Serrao [a], Walter Bertoldi [a,b], Simone Bizzi [c], Alfonso Vitti [a], Christoph Hauer [d], Klodian Skrame [e], Bestar Cekrezi [a], Guido Zolezzi [a,b]

[a] Department of Civil, Environmental and Mechanical Engineering, University of Trento, Italy
[b] Center Agriculture Food Environment, University of Trento, Italy
[c] Department of Geosciences, University of Padua, Italy
[d] Institute of Hydraulic Engineering and River Research, University of Natural Resources and Life Sciences, Wien, Austria
[e] Department of Applied Geology Environment and Geoinformatics, Polytechnic University of Tirana, Albania

ARTICLE INFO

Keywords:
Vjosa river
River morphological trajectories
Climatic control
System relaxation
Free-flowing rivers
River management

ABSTRACT

Free-flowing rivers (FFRs) are fundamental references for river management, providing the opportunity to investigate river functioning under minimal anthropic disturbance. However, large free-flowing rivers are rare in Europe and worldwide, and knowledge of their dynamics is often scarce due to a lack of data and baseline studies. So far, their characterization is mainly grounded in the longitudinal connectivity assessment, with scarce integration of further hydro-morphological aspects, particularly concerning the processes and drivers of changes in their morphology over time scales of management relevance. This work aims to broaden the characterization of FFRs by reconstructing their catchment-scale morphological evolutionary trajectories and understanding their driving causes, to support their management better. This is achieved by integrating freely available global data including Landsat imagery and climatic reanalysis with the few locally available quantitative and qualitative information. The analysis of possible drivers of change at the catchment and reach scale assesses hydrological variability, flow regulation, land use change, sediment mining and bank protection works. We applied this approach to the Vjosa River (Albania), a model ecosystem of European significance and one of the few FFRs in Europe. The Vjosa was recently declared a Wild River National Park. We investigated its catchment-scale morphological changes over 50 years, considering four reaches of the Vjosa and four reaches of its main tributaries. Satellite imagery was analyzed taking advantage of Google Earth Engine cloud computing platform. The analysis reveals a catchment-scale response to climatic fluctuations, especially in the most natural reaches, with a significant narrowing of the active river corridor, following a flood-intense period in the early 1960s. The narrowing rate gradually decreased, from 35% before 1985 to 24% between 1985 and 2000, reaching a new equilibrium from 2000 to 2020. However, the recent trajectories of the lowland reaches have been impacted by human pressures, particularly sediment mining, which intensified after the 1990s, suggesting that these reaches may instead be far from equilibrium and adjusting to such persistent stressor. Identifying the key drivers of change and building catchment-scale knowledge of geomorphic change can inform the management of riverine protected areas, and the proposed integrated approach is a promising tool to help overcome the data scarcity typical of the limited remaining large FFRs.

1. Introduction

Global interest in the world's remaining free-flowing rivers (FFRs) has increased rapidly (Grill et al., 2019) because they are associated with high ecological integrity and natural value. This comes along with the recognition of the dramatic decline in freshwater biodiversity (Tickner et al., 2020; Albert et al., 2020), which is closely associated with the growing extent of river fragmentation and regulation (Belletti et al., 2020). Present and projected human stressors are however of high concern for several large rivers that still show free-flowing reaches (e.g. Best, 2019), putting their ecological integrity and related ecosystem services at risk (Young et al., 2022). River systems with larger

* Corresponding author.
E-mail address: marta.crivellaro@unitn.it (M. Crivellaro).

https://doi.org/10.1016/j.jenvman.2024.122541
Received 19 January 2024; Received in revised form 4 July 2024; Accepted 10 September 2024
Available online 2 October 2024

catchments offer more opportunities for regulation and exploitation, and therefore large free-flowing rivers are particularly rare and endangered.

Free-flowing rivers have essentially been defined in terms of their longitudinal hydrological connectivity (e.g. Grill et al., 2019), but much less emphasis has been placed on other key features that sustain ecosystem health. Among these features, the sediment supply regime, sediment connectivity, and lateral connectivity are of recognized relevance (e.g. Wohl et al., 2015; Wohl, 2017). Indeed, alterations of the sediment supply regime are crucial for the morphological pattern and dynamics, which ultimately regulate flood risk, sustain the availability and diversity of natural habitats, and thus the unique biodiversity and ecosystem functions of FFRs. Furthermore, the lateral connectivity reveals "how large" river reaches are (Gurnell et al., 2016), and therefore defines the space needed for the natural functioning of a multitude of interaction processes between the active river corridors and the surrounding areas. Managing FFRs to maintain their ecological integrity and ecosystem value, preserving their free-flowing character, therefore requires broadening the quantitative characterization of FFRs, presently based mainly on their longitudinal hydrological connectivity, to account for lateral connectivity and geomorphic processes.

In developing and emerging countries, where most larger FFRs can still be found, anthropic effects on river geomorphic processes and sediment regimes are of increasing concern, because rapid social and economic development causes increasing alterations (Zarfl et al., 2015). Very few large free-flowing rivers remain in continental and Mediterranean Europe (Tockner et al., 2009; He et al., 2021), with exceptions mainly in the Balkan region. Also, these last European FFRs are facing rapid human exploitation with the development of hydropower projects, channelization and large-scale sediment mining (Wagner et al., 2019; Carolli et al., 2023). Such interventions are often proposed with inadequate environmental impact assessments and without the hydro-morphological and ecological information needed to properly assess their sustainability. Uncontrolled exploitation and associated hydromorphological alterations occur in the Balkan region despite a growing number of international studies highlighting the area as "the blue heart of Europe", with a high density of almost intact river systems of continental relevance, very rich in biodiversity and ecosystem services (Eco-Masterplan for Balkan rivers, 2018). Recent studies on the Vjosa river, for example, show that 86% of the habitats in its river corridor can be associated with threatened biota as listed in the EU Habitats Directive (Schiemer et al., 2020). Moreover, the Vjosa river hosts taxa that have been discovered only recently in science (Graf et al., 2018), together with many species that were once abundant in European river corridors but are now rare and endangered (Schiemer et al., 2018). FFRs are therefore highly precious also for science, as they offer almost unique and increasingly rare opportunities to observe and investigate riverine processes as they would occur under minimal anthropic pressure (Ward et al., 1999; Schiemer et al., 2020). For analogous reasons, they also represent fundamental references for setting environmental targets in river management, in particular for river restoration (e.g. Kondolf and Zolezzi, 2008 European CommissionDirectorate-General for Environment, 2022), biodiversity conservation (e.g. Brasseur et al., 2023) and preservation of ecosystem services (Auerbach et al., 2014). However, the management of FFRs for preserving their multiple values poses specific challenges that may require dedicated, specific regulatory frameworks (e.g. the Wild and Scenic Rivers Act in the USA and the Rapid Protection Act in Finland). A major limitation is the frequent lack of data, with particular reference to morphological evolution and geomorphic processes, which determine the physical template of the river system functioning at different spatial and temporal scales and regulate the biodiversity and ecosystem services they can provide.

Increasingly used indicators to quantify how the morphology of a river reach has responded to alterations of the flow and sediment supply regimes, and to direct modifications of its planform, are the so-called morphological evolutionary trajectories (Brierley et al., 2002; Brierley and Fryirs, 2005, 2016; Surian et al., 2009; Beechie et al., 2010; Grabowski et al., 2014). They support decision-making in river management, especially when associated with an analysis of their causal factors, of both natural or anthropic origin. Anthropogenic causal factors often relate to multi-scale modifications of the flow and sediment supply regimes, which are the focus of most management decisions (Liébault and Piégay, 2002; Surian and Rinaldi, 2003; Comiti et al., 2011). These factors act at different time and space scales. Land use change, dams and diffuse torrent control works (Lach and Wyżga, 2002; Kiss and Blanka, 2012; Scorpio and Piègay, 2021) are the main drivers at the catchment scale, while channelization and other control structures influence channel dynamics at the reach scale (Scorpio et al., 2015, Hohensinner et al., 2018). Other stressors, such as sediment mining, affect river morphology at multiple scales, both of the reach in which they occur and of multiple reaches in the catchment through regressive or progressive channel incision (Kondolf, 1997; Surian et al., 2009; Martín-Vide et al., 2010). Natural control factors such as climate and flood occurrence also influence river trajectories (Wyżga, 2007; Batalla et al., 2018; Comiti et al., 2011). Large floods (Belletti et al., 2015), as well as changes in temperature and precipitation (Comiti, 2012; Coulthard and Van de Wiel, 2013) and riparian vegetation (Gurnell et al., 2012) may have effects at the reach to catchment scale. Interpreting morphological trajectories in the light of specific causal factors is however challenging because the effects of natural and anthropogenic stressors often overlap on similar time scales (Surian, 2022). Explanation of inference of geomorphic change has been mostly proposed for rivers subject to strong human modifications (Surian and Rinaldi, 2003; Zawiejska and Wyżga, 2010; Armaş et al., 2013; Arnaud et al., 2019; Surian, 2022), while much less is known about the morphological trajectories, and their drivers, typical of FFRs.

In this work, we aim to show how understanding the morphodynamic evolution of FFRs can be relevant for their management. To this aim, we assess the morphological trajectories together with their natural and anthropogenic drivers, referring to a case study of recognized international relevance: the free-flowing Vjosa river in Albania, and expanding the set of indicators used so far to characterize FFRs. The Vjosa river is a reference for the Balkans and also for Europe, and it was recently declared the first Wild River National Park in Europe (Karen McVeigh, 2023). Currently an important process is underway to define the boundaries and specific characteristics of such a highly valuable protected area, for which information on the active river corridor width and of its historical evolution is crucial.

We propose an innovative approach to study the evolutionary trajectories, which we analyze from the reach scale (on 8 reaches) to the catchment scale over 50 years (1968–2020). The approach also addresses the limited data availability, often found when dealing with FFRs, and incorporates recent advances in the integration of geomorphology, geomatics and remote sensing (Carbonneau and Piegay, 2012; Bizzi et al., 2015; Spada et al., 2018; Piégay et al., 2020; Boothroyd et al., 2021a) with cloud computing resources (Boothroyd et al., 2020, 2021b; Vercruysse and Grabowski, 2021; Crivellaro et al., 2024) and combining streamflow and rainfall reanalysis data.

2. Materials and methods

The proposed approach is based on i) reconstructing the recent (60 years) morphological trajectories of selected homogeneous river reaches; and ii) analysing the possible drivers of change at the catchment and reach scales. To reconstruct the river morphodynamics, we analyze multi-temporal satellite images from different sources and extract relevant indicators of the morphological trajectories, while we attempt to quantify hydrological and land cover changes, the presence of river impoundments and of sediment mining in the river channel as possible drivers of river morphodynamics, addressing the constraints posed by limited data availability. In this section, we briefly describe the study area, followed by a detailed description of each implemented method.

2.1. Study area

The Vjosa river originates at the base of the Pindos mountains (GR) and extends over 272 km from its sources, through the south of Albania to the Adriatic Sea, with a total catchment size of 6704 km^2. Flowing in a SE-NW direction, the river is joined by several tributaries; among them, the most relevant are Voidomatis (GR), Sarandaporo (GR/AL), Langarica (AL), Drinos (AL), Bënçë (AL), Shushica (AL) (see Fig. 1 for tributaries location). Climate shifts downstream from Alpine to Mediterranean and the hydrological regime is pluvio-nival with characteristic floods in autumn and late winter-spring. Specifically, around 66% of the flow originates from rainfall, while between 21% and 25% come from snowmelt, and the residual represents baseflow (Skoulikidis et al., 2022). The basin has a high stream density (0.92 km/km^2) and high runoff coefficient (0.95) due to the dominance of flysch (Skoulikidis et al., 2022). Limestones (≈25%), clastic sediments (17%), sandstones (8%), metamorphic rocks (2%) and igneous rocks (less than 1%) are also present. As reported by Hauer et al. (2019), such geological composition and variety lead to the high loads of suspended sediments in Vjosa's mainstem. Sediment transport in the central course of the Vjosa river, near the village of Pocem, was recently determined as 5 million tonnes/year with a bankfull discharge of approximately 1000 m^{3}s^{-1} (Hauer et al., 2019).

Our study focuses on eight reaches with different morphology and confinement status (see Fig. 1 and Table 1). We analyzed four reaches along Vjosa's main course (V1, V2, V3, V4) and four along its main tributaries (Sarandaporo T1, two reaches along the Drinos river T2, T3, Shushica T4), proposing a reach-scale approach to analyze the behavior of the morphological trajectories at the catchment scale.

Prior to reach selection, the first phase of the IDRAIM multiscale hierarchical framework (Rinaldi et al., 2015) was applied to the Vjosa river system to characterize it from the catchment to the reach scale, using the 2015 ASIG national orthophoto as a baseline information (Fig. 1). The procedure consists of: the definition of the three main Physiographic Units (Mountain, Hill, Lowland); the delineation of the river floodplain and the partitioning the main stem of the Vjosa river into four river segments. After that, lateral geological confinement is assessed for each segment through a "confinement index" and a "confinement degree" (Rinaldi et al., 2015). This eventually resulted in the subdivision of the Vjosa river into hydro-morphologically homogeneous reaches, from which the 8 target reaches listed above were selected. The choice was restricted to unconfined or partially confined reaches, which are free to adjust their width, allowing to capture morphological planimetric variations. Only reaches with an average corridor width (defined as the river corridor area by reach length ratio, see Table 1) greater than 150 m were considered, to allow proper identification of the river corridor planform classes (water, bare sediments, vegetation) from medium resolution remote sensing images.

Aerial images of the 8 reaches are reported in Supplementary Materials S1; Table 1 presents their main morphological characteristics.

2.2. Recent morphological trajectories

To analyze recent morphological trajectories of the Vjosa river at the catchment scale, we combined:

i) for all reaches, the extraction of active width over time from two remote sensing data sources, considering as input data both Landsat collections and USGS Corona declassified imagery. Corona images are declassified products from American military satellite systems

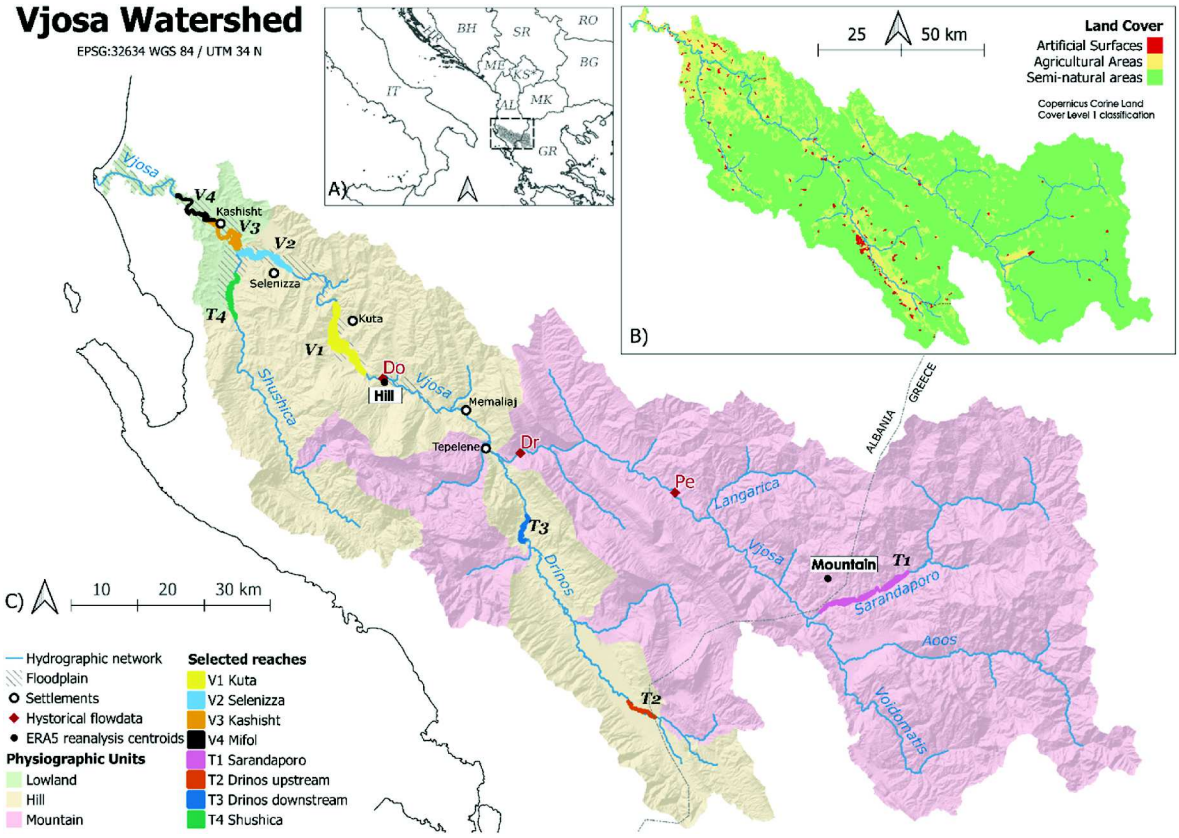

Fig. 1. A) Location and map of the Vjosa river catchment, B) Catchment land cover map (Corine 2018 - Level1) C) indication of hydrographic network with main lateral tributaries, historical gauging stations considered in this study (Permet-PE, Dragot-DR, Dorez-DO), physiographic units (Mountain, Hill, Lowland), floodplain and selected river reaches (V1, V2, V3, V4, T1, T2, T3, T4: see Table 1 for more details), ERA5 reanalysis considered centroids (up, low). Hillshade basemap refers to the EuDem elevation model.

Table 1
General description of selected reaches. Confinement (U = Unconfined and PC= Partially Confined) and Morphology classes (M = Meandering, S= Sinuous, T = Transitional, W=Wandering, B=Braided) follow IDRAIM classification (Rinaldi et al., 2015). The sinuosity Index (Is) has been reported only where relevant to characterize unconfined and partially confined morphologies. Specific stream power ω (W/m^2) is calculated at the reach scale considering as reference discharge the 99.9 percentile (recurrence time of 2.7 years) obtained by Bizzi et al. (2021), using LISFLOOD distributed hydrological model for the Vjosa catchment.

Reach Name	Distance from the sea (km)	Average reach elevation	Reach length	River corridor area	Channel Slope	Confinement	Morphology 2015 orthophoto	Average active width (2020)	Sinuosity 2015 orthophoto	Specific stream power ω
		m. a.s.l.	(km)	(ha)	(m/km)			(m)	Is (–)	(W/m^2)
Kuta V1	62.4	53	13.5	1268.9	1.8	PC	B	500	–	43.4
Selenizza V2	38	12	12.3	722.6	1.3	PC	S/T	300	1.32	54.4
Kashisht V3	27.5	5	12	555	1.1	U	S	200	1.78	83.1
Mifol V4	19.2	2	10.5	259.5	0.2	U	M	70	1.73	42.7
Sarandaporo T1	175	605	16.4	561.5	3.3	C	B	200	–	28.4
Drinos upstream T2	156.1	205	6.3	93.7	3.4	PC	T	100	–	37.4
Drinos downstream T3	115.3	165	5.8	139.2	1.8	C	W	150	–	41.3
Shushica T4	43.8	35	8.1	347.4	2.2	PC	W	200	1.21	20.1

which acquired photographic images from space in the 1960s and 1970s;

ii) for lowland reaches, the assessment of river morphology variation considering the sinuosity index and expert judgment in the comparison of 1968 Corona images and 2015 orthophoto.

2.2.1. *Landsat analysis method*

In this work, Google Earth Engine (GEE) was used to extract information on river planform morphodynamics from multi-temporal, multispectral, medium spatial resolution (30 m) satellite imagery, namely Landsat Surface Reflectance products (Landsat 5 Thematic Mapper, Landsat 7 Enhanced Thematic Mapper, and Landsat 8 Operational Land Imager).

The implemented morphological assessment procedure used a combination of the normalized difference vegetation index (NDVI) and the modified normalized difference water index (MNDWI) (Xu, 2006) to extract the active channel and the vegetation cover. Fig. S3 reports the detailed workflow of the procedure. The active channel is here defined as the region of the domain showing recent hydromorphological activity, i.e., the area that includes bare sediments and low-flow channels, following previous work (Henshaw et al., 2013; Monegaglia et al., 2018; Spada et al., 2018; Boothroyd et al., 2020, 2021a; Harezlak et al., 2020).

We selected a time resolution of 5 years, for a total of eight observations from 1985 to 2020. Per each observation, we considered the collection of all available Landsat images in the year of observation. Then, we computed per each image of the collection the NDVI and MNDWI maps. For the two multispectral indexes collections, a synthetic image representative of the observed year was computed, applying a median reducer to aggregate all spatially overlapping non-cloud pixels, as proposed by Crivellaro et al. (2024). Thus, the annual active channel (ACy) was mapped with relational operators applied to the two synthetic images. Specifically, MNDWI $\geq$ -0.35 (Boothroyd et al., 2020) and NDVI $<$0.15 (Bertoldi et al., 2011) were the conditions for active channel masking. The domain of analysis (EM mask) for each reach was then defined as the envelope computed from the eight ACy. A detailed description of the procedure is reported in Crivellaro et al. (2024).

To map the dynamics of the riparian vegetation, we limited the image collection of each year to the vegetation growing season (May to October in the northern hemisphere), and we extracted and analyzed active channel changes considering the growing season derived data as the reference for planform dynamics. Analogously to the annual active channel computation, a synthetic median image for both NDVI and MNDWI were produced. Inside the domain envelope (EM mask), pixels were classified as active channel (AC) when NDVI was $<$0.15, vegetation (VEG) otherwise. The EM mask per each river reach, along with the seasonal active channel and vegetation maps were exported from Google Earth Engine and processed through GRASS GIS software. A single reference centerline was extracted from the domain envelope (v.voronoi) and used to generate cross-sections (v.transects) at 300 m intervals (as in Jézéquel et al., 2022).

Finally, we processed the obtained maps to assess two morphological indicators:

i) "*Active width*", as the width of the active channel in each reach cross-section per each year of observation.

ii) "*Vegetation %*" cover, as the percentage of the vegetation within the total reach active channel envelope in the observed year.

The accuracy of the semi-automatic procedure has been assessed by computing the percentage of difference in terms of active channel area between the available 2015 Orthophoto (by means of expert manual digitalization) and the 2015 active channel mask derived from Landsat Images. Since the Landsat resolution is 30 m, the range of applicability of the *active width* extraction should prefer "large" rivers, for which an acceptable error could be achieved (Monegaglia et al., 2018). In the

Vjosa case study, the average river corridor width of selected reaches goes from 1 km (V1 Kuta reach, 33 times pixel resolution) to 150 m (T2 Drinos upstream, 5 times pixel resolution). Considering this, the expected misclassification error ranges from 3 to 20%.

2.2.2. Corona analysis method

The first generation of US photographic reconnaissance satellites (Corona, Argon and Lanyard) collected more than 860,000 images of the Earth's surface between 1960 and 1972. Already in 1992, the use of such early satellite data for environmental studies was evaluated. In 1995, the images were declassified and are now publicly accessible. Since then, a plethora of studies have used these products for environmental and historical studies.

Four medium-resolution grayscale Corona Images acquired on December 12th' 1968 were added to the analysis to extend the investigated time interval. Images covered only 6 of the studied reaches: V1 Kuta, V2 Selenizza, V3 Kashisht, V4 Mifol, T2 Drinos upstream and T4 Shushica. The remaining two reaches were not fully included in the surveyed area or there was excessive cloud coverage. Each image was georeferenced using 9 GCPs identified on a 2015 orthophoto (available as WMS through the State Authority for Geospatial Information - ASIG platform) with a second-degree polynomial transformation and nearest neighbor resampling (Table S2), and a spatial post-georeferenced spatial resolution of 2.5 m.

Manual active channel digitizing was performed on a GIS (QGIS 3.10) for each of the six georeferenced reaches, producing the active channel masks. Analogously to the Landsat GRASS-based procedure, longitudinal distributions of active channel widths were computed.

2.2.3. Relative variation of the active width

To outline the system's response in terms of narrowing or widening, we evaluated the *relative active width variation* (Wr) for three time periods of comparable duration. These were identified by i) considering the available input data sources (Corona or Landsat images) and ii) ensuring a comparable number of observations in the two periods covered by Landsat data. The first period covers 1968 to 1985, for the reaches where the Corona images were available, the second and third periods are 1985–2000, and 2005–2020.

The relative active width variation for the i-th cross-section $(W_{r,i})$ was defined as:

$$W_{r,i} = \frac{W_{start,i} - W_{end,i}}{W_{start,i}} \quad (1)$$

where $W_{start,i}$ is the width in the starting year and $W_{end,i}$ is the width in the last year of each period, for the i-th cross-section.

2.2.4. Assessment of variations in the river morphology

Morphological variations have been further assessed by integrating expert judgment in the morphological classification of reaches with the analysis of sinuosity variation over time in lowland reaches (V2, V3, V4, T4), using the 1968 Corona Images and the 2015 Orthophoto as input data.

2.3. Hydrological analysis

2.3.1. Discharge time series analysis

The historical discharge data have been collected by the former Hydrometeorological Institute of Albania. They refer to the gauging stations of Permet (PE) and Dragot (DR) in the upper catchment (monthly data from 1969 to 2000 and 1948 to 1990, respectively) and of Dorez (DO, daily data from 1958 to 1990). The locations of the gauging stations are mapped in Fig. 1. Firstly, a discharge time series analysis was conducted at a monthly scale. Permet, Dragot and the aggregated Dorez data were all normalized to compare their dimensionless evolution over time and to qualitatively test their consistency. Normalization was performed by subtracting the average value $\underline{x}$ and dividing by the standard deviation σ of each record. Then, a daily scale analysis was carried out for the Dorez not-normalized record to evaluate the duration, frequency, and magnitude of flood events that are likely to produce an effect on the active channel width. We defined these flood events as having discharge above two thresholds with known geomorphic relevance: the initiation of bedload transport and the bankfull discharge. These values were obtained for the reach of Dorez hydrometric station through direct bedload measurements (Hauer et al., 2021) and through standard hydraulic computations (e.g. Schiemer et al., 2020): $Q_{bt} = 350$ m^3s^{-1} for bedload initiation and $Q_{bf} = 1000$ m^3s^{-1} as the bankfull discharge. To detect statistically significant trends, Mann Kendall trend test was performed, using Python PyMannKendall module. A statistical analysis of the return interval of major flood events has been performed by assuming that the distribution of the recorded series of events over bankfull discharge Q_{bf}, in Dorez, from 1958 to 1990, follows a Gumbel distribution.

2.3.2. Rainfall reanalysis and precipitation-discharge correlation

To overcome data paucity and the unavailability of measured hydrological data (discharges and rainfalls), we included in our study a long-term (1950–2020) rainfall analysis using ERA5 total precipitation rainfall reanalysis (Hersbach et al., 2018; Bell et al., 2021), downloaded from the Copernicus Climate Change Service (C3S) Climate Data Store. The data cover the entire globe and are provided in a regular latitude-longitude grid projection, with a horizontal resolution of 0.25°.

Precipitation values were spatially filtered within the Vjosa catchment region of interest and then aggregated in two areas: the upper watershed (centroid coordinates: 40.125 N, 20.625 E), corresponding mainly to the mountain physiographic unit, and the lower watershed (centroid coordinates: 40.386 N, 19.836 E).

A spatial average value of hourly precipitation was computed for the two areas, as the rainfall indicator for the entire area. The obtained time series were aggregated into monthly and annual cumulative values, normalized using the same approach applied to discharge data, and compared with them. As Dorez and Permet stations are located in the upper watershed, upper cumulative values have been considered as contributing rainfalls for both DO and PE subcatchments. For Dorez station, we computed a spatially weighted rainfall time series, with weights reflecting the proportion of the two contributing areas in the Dorez subcatchment (76% in the upper watershed and 24% in the lower watershed).

Rainfall and discharge data of each station have been correlated, expressed as 12-month moving average. Moreover, Mann Kendall trend test on cumulative monthly values was computed to study the general trend of rainfalls, in comparison with Dorez discharge trends.

Annual river runoff volumes were computed for the three gauging stations by time integration of the related monthly discharge time series. These amounts were then normalized and compared to the normalized annual rainfall volumes, thus testing the river annual flow's dependency on climate variability by looking at the annual anomalies.

2.4. Analysis of human stressors

We evaluated the effect of human stressors at different spatial (reach to catchment) and temporal scales (years to decades), to analyze the possible impact of land use change, dam construction, sediment mining and riverbank structures on the river morphological evolution.

The spatial and temporal variation of forest cover in the Vjosa catchment from 1986 to 2020 was assessed using a Landsat-based method. Due to the scarcity of historical data, medium-resolution Landsat imagery was considered the most appropriate source to assess forest cover dynamics over the last decades, conversely to more classical approaches based on historical maps and orthophotos. Firstly, a supervised land cover classification was implemented. A synthetic, growing season (May to October) representative image of 1986 was computed

using Landsat.simpleComposite GEE command, over which a supervised classification was applied. Two classes were identified: forest and non-forest, using a set of 100 training pixels. Then, to assess the progressive forest change from 1986, we used the LandTrendr algorithm (Kennedy et al., 2010), which employs the Landsat-based detection of trends in disturbance and recovery algorithm to generate a simplified pixel-based spectral-temporal forest cover trajectory. The model output considered in this study was the spatially explicit data on forest loss and recovery with embedded information of the year of disturbance, allowing to detect spatial and temporal patterns in net forest loss (loss minus recovery) within the catchment.

The occurrence and extent of sediment mining sites and riverbank protection were mapped from Google Earth freely available imagery. Due to the coarse resolution of satellite images in the 1980s and the 1990s, such sites were detectable only starting from 2004. Gravel sieve machines detected from Google Earth were mapped through expert judgment along the entire river corridor, considering the entire river network reported in Fig. 1. Per each sieve, we mapped the visible extent of the affected sediment mining area, recognizing typical planimetric forms associated with river sediment mining, such as localized pits and pools, temporary in-channel roads, man-made gravel embankments, and service areas. Analogously, riverbank structures were mapped, such as embankments and groynes, detectable from 2004 until nowadays (see Supplementary Material S4 for evidence of sediment mining and riverbank protections). To qualitatively assess sediment mining activities and riverbanks before 2004, Corona images (1968) were also considered, where available. Moreover, interviews with local stakeholders have been done to understand the likelihood of sediment extraction pressure in the 1968–2004 period.

The assessment of hydropower plants (HPPs) within the Vjosa watershed is based on Euronatur – RiverWatch – Fluvius 2020 Database (EuroNatur, Riverwatch, FLUVIUS), which reports the ensemble of operating, under construction, and planned structures for the entire Balkan Region. The database was filtered for the Vjosa catchment, and

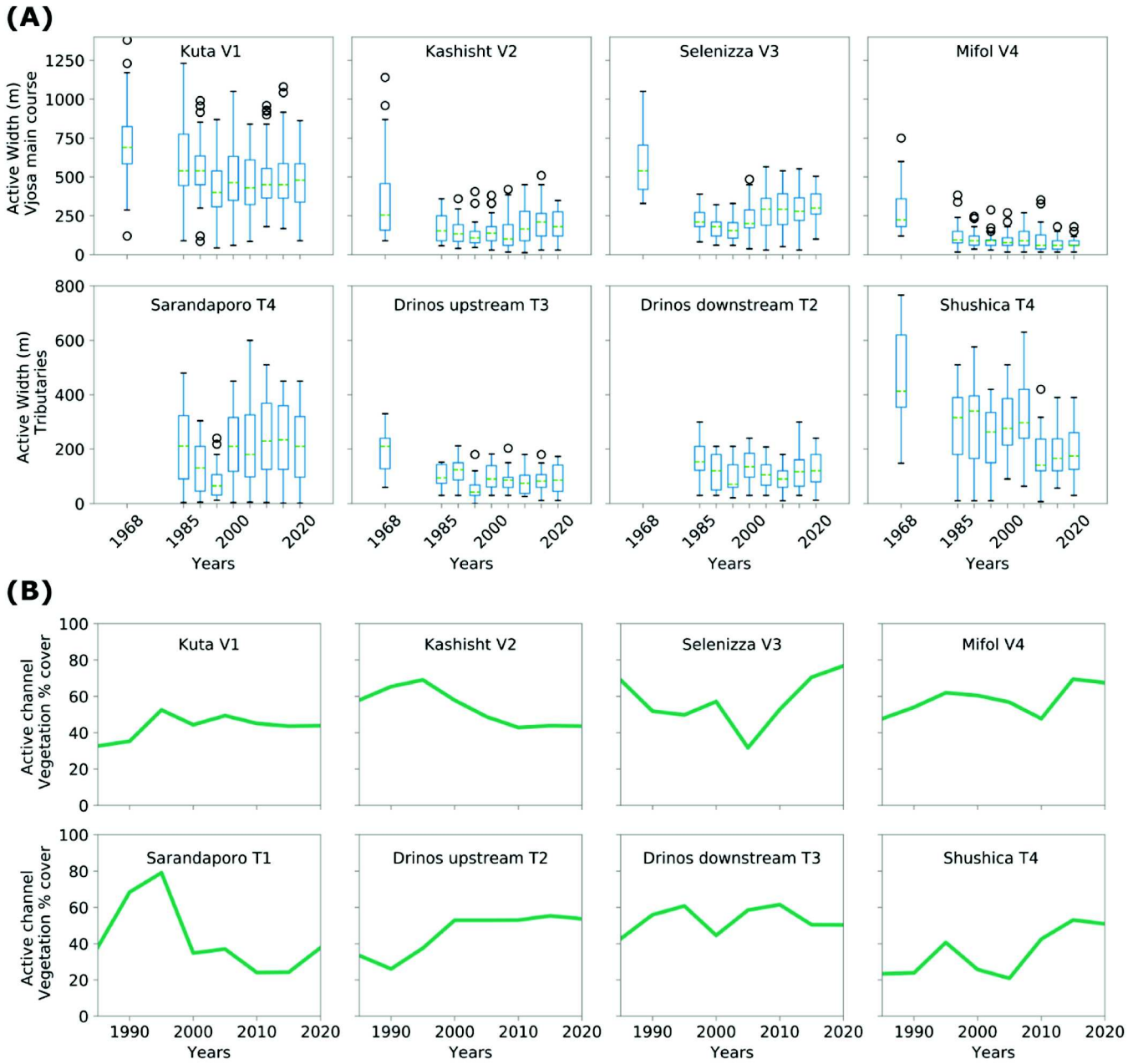

Fig. 2. Time variation of (A) the active width distributions and of (B) vegetation % cover in the eight study reaches.

only long-term operating HPPs (>10 MW operating since more than 35 years) with a storage reservoir were considered. The majority of dams are located in mountain tributaries of the Vjosa river. Hydropower Plants are mainly run-of-rivers type with none or small (daily regulation) reservoirs. They are mostly of very recent construction (not older than 10–15 years, impounding 15% of the catchment). Pigai Aoos Hydropower Plant (Pigai HPP, Epirus, Ioannina prefecture) results from the filtering process, with potential influences on the hydromorphological trajectory of the system, where an artificial lake (260 Mm^3) was created in 1984 at the subalpine plateau (1400 m.a.s.l., impounding 1% of the total Vjosa catchment), diverting around 10% of Vjosa headwaters toward the Arachthos basin since 1987, with an installed power of 210 MW (Public Power Corporation S.A., 2016). While the impact on the flow regime of Pigai HPP in the Greek part of Vjosa has already been investigated (Leontaritis and Baltas, 2014), no study is known regarding its influence in the Albanian part of the river. Considering available data, Pigai HPP's impact on the flow regime of the Albanian part of the Vjosa river has been assessed by applying Pettitt's test for single change point detection to Permet historical data (1969–2000). Specifically, it has been applied on seasonal streamflow volumes over time in Permet, expressed as average monthly volumes (March for the rainy season and September for the dry one were chosen), and to annual discharge

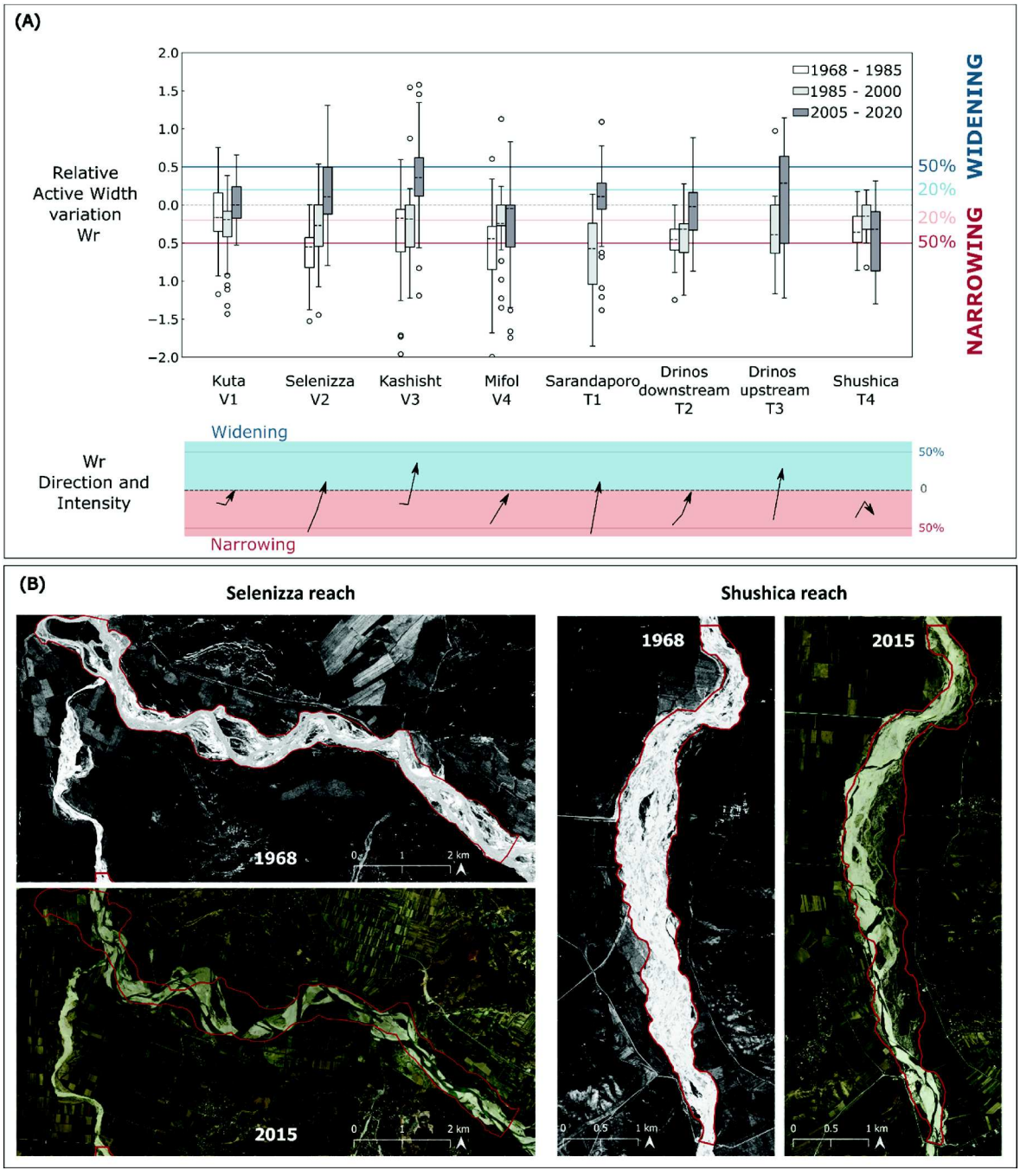

Fig. 3. (A) Relative active width variation Wr derived from Corona (where available) and Landsat scenes from 1968 to 2020 for the analyzed reaches are plotted separately for three reference periods: 1) 1968–1985, 2) 1985–2000, 3) 2005–2020. Light and dark blue (red) thresholds represent 20% and 50% widening (narrowing) with respect to the reference year. The direction and intensity vectors in the lower panel link Wr median values per each period. (B) V2 Selenizza and T4 Shushica reaches in the 1968 Corona images and in the 2015 Orthophoto. The red lines delimit the active channel in 1968. (For interpretation of the references to colour in this figure legend, the reader is referred to the Web version of this article.)

volumes. Once the potential change point has been identified, the Kolmogorov–Smirnov statistic (Smirnov, 1939) was applied to the two series, before and after the potential change point.

3. Results

3.1. Recent morphological trajectories

3.1.1. Active width

Active widths extracted from Corona and Landsat images were analyzed to describe the recent morphological trajectories of the system (Fig. 2A). A general narrowing trend can be noticed with reference to 1968. Narrowing is particularly evident along the Vjosa main course. From 1968 to 2020, the median active width of the 4 reaches located on the Vjosa main stem decreased from 225 m to 60 m in Mifol V4, from 255 m to 180 m in Kashisht V3, from 540 m to 300 m in Selenizza V2 and from 690 to 480 m in Kuta V1. Narrowing is also visible in two of the tributaries, with Drinos upstream T2 and Shushica T4 narrowing from 210 m to 86.5 m and from 316 m (in 1985) to 174 m, respectively. Conversely, Sarandaporo T1 and Drinos downstream T3 show no significant overall changes in active width. It is relevant to notice that Kashisht V3, Selenizza V2 and Sarandaporo T1 reaches show an initial phase of narrowing until the late 90s, followed by a recent widening of the active channel. Applied Mann-Kendall trend test with $\alpha = 0.05$ shows no statistically significant trend in active width variations of the selected reaches, except for Mifol V4 and Shushica T4, which show a significant decrease in maximum (p-value = 0.045 and 0.034, respectively) and average active width (p-value = 0.003 and 0.034, respectively).

Fig. 2B reports an increasing trend in vegetation % cover in V4, V2, T4 and T2 reaches, associated with the narrowing of the active channel. Other reaches show no visible change in vegetation cover to the total envelope area, except for T1 and V3, which present a decreasing trend in vegetation cover compared to the 1990s.

Fig. S6 outlines the relative change in active width compared to the width in 1985 for each year of observation of the Landsat imagery. Channel narrowing can be observed in all reaches, with a similar trend until 2000, while in the last 20 years river reaches present a more diverse morphological response. Considering the entire observed trajectory (Fig. 3A), it is possible to appreciate greater narrowing intensity in the first period, where median relative narrowing rates vary from 16 to 54%. The same reaches showed reduced narrowing rates in the second period (1985–2000) compared to the first period(1968–1985: 18%–31%). As for the last period (2005–2020), the narrowing rates decreased for the majority of the reaches (1% to −11%) and even switched to widening in the case of V3 (35% median widening) and T3 (25% median widening). The only exception to this trajectory is the T4 reach, where narrowing rates increased in the last period (40% median narrowing).

Landsat semi-automatic accuracy assessment delineated an error range of 3–8% for the selected reaches, from a 3% relative error for the widest Kuta V1 reach to 7% and 8% errors for the narrower Mifol V4 and Drinos downstream T3 reaches, respectively. An exception is the case of the Drinos upstream T2 reach, which presents a 20% error due to an underestimation of the active channel mask linked to the impossibility of calibrating the local NDVI threshold for vegetation classification and because of the relatively small width of the reach compared to the resolution of the Landsat imagery. Nevertheless, assuming such underestimation as constant over time, the trajectory of the active channel can still be considered a valid indicator of the morphological evolution of the reach.

Table 2
Sinuosity index variation in the lowland reaches of the Vjosa river system from 1968 to 2015.

Reach Name	Sinuosity (Is)		Morphology	
	1968	2015	1968	2015
Selenizza V2	1.13	1.32	W	S/T
Kashisht V3	1.52	1.78	M	M
Mifol V4	1.65	1.73	M	M
Shushica T4	1.15	1.21	B	W

3.1.2. River morphology assessment

A change in the morphological pattern from 1968 to 2015 was visible only for some of the lowland reaches, while the ones in the hill and mountain landscape units kept the same morphology, despite variations in their active width. More specifically, the sinuosity index increases over time, for all considered lowland reaches (V2, V3, V4, T4) reported in Table 2. The combination of a reduction in the active width and an increase in the sinuosity, together with qualitative morphological observations on bars and vegetated islands as visible in the 1968 and 2015 images, indicates a clear shift of the lowland reaches towards a more sinuous, single-thread channel morphology. V2 Selenizza reach, which was classified as a wandering morphology in 1968, is nowadays approaching a sinuous pattern, where the areas with a multichannel behavior disappeared almost completely (Fig. 3B). Similarly, Shushica T4 reach experienced a large decrease in channel width, coupled with a drastic reduction in the number of anabranches, moving from a braided configuration to a wandering pattern.

3.2. Hydrological analysis

3.2.1. Discharge analysis

The aggregation of the original Dorez daily streamflow series at monthly scale and then the normalization of the three monthly series (including Dragot and Permet) allows the comparison of the monthly variations in normalized streamflow at the three stations, which shows satisfactory consistency in their overlapping periods (Figs. S7–B). Such consistency, especially for monthly low flow conditions, is also evident in the pairwise scatter plots of normalized streamflow values (Fig. S7-C, D, E). Daily historical records of Dorez station report a maximum peak value of 3140 m^3s^{-1} in early 1963 and lowest flows as 15 m^3s^{-1}, with a mode of 40 m^3s^{-1} (Figs. S7–A).

To better connect the analysis of the flow records with the observed morphological trajectories, we focused on analyzing the properties of flow events above the sediment mobility and bankfull thresholds. Precisely, the peak discharge, number and duration of events above the thresholds were computed for each month and plotted over time (Fig. 4). The Mann Kendall trend test ($\alpha = 0.05$) outlined that the decreasing trends in duration and frequency of flow events above the sediment mobility and bankfull thresholds are statistically significant (above Q_{bt}, p-value_duration = 0.033, p-value_freq = 0.0033; and above Q_{bf}, p-value_duration = 0.033, p-value_freq = 0.0073; Fig. 4B, C, D, E, see Table S8 for additional information). Instead, temporal trends in peak discharges are not statistically significant (Fig. 4A).

3.2.2. Rainfall reanalysis and precipitation-discharge correlation

Mann Kendall trend test ($\alpha = 0.05$) was also applied to the time series of monthly cumulative rainfalls derived from ERA5 total precipitation data. Analyzing the period for which Dorez daily flow rates are available (1958–1990), a decreasing trend can be noticed both in the rainfall time series (p-value in the mountain area <0.001, p-value in the hill area = 0.005) and in the monthly cumulative flows (p-value <0.001, further information in Table S9).

A strong correlation appears (Tau rank $\tau = 0.73$) between contributing weighted rainfalls and Dorez discharges in the period 1958–1990 (expressed as 12-month moving average time series; more details in Fig. S10). Analogously, a correlation emerges between precipitations in the mountain area and the streamflow series in Permet ($\tau = 0.58$) and Dragot ($\tau = 0.59$).

Therefore, climatic trends shown by two monthly and one daily flow records in three different hydrometric stations are highly coherent with

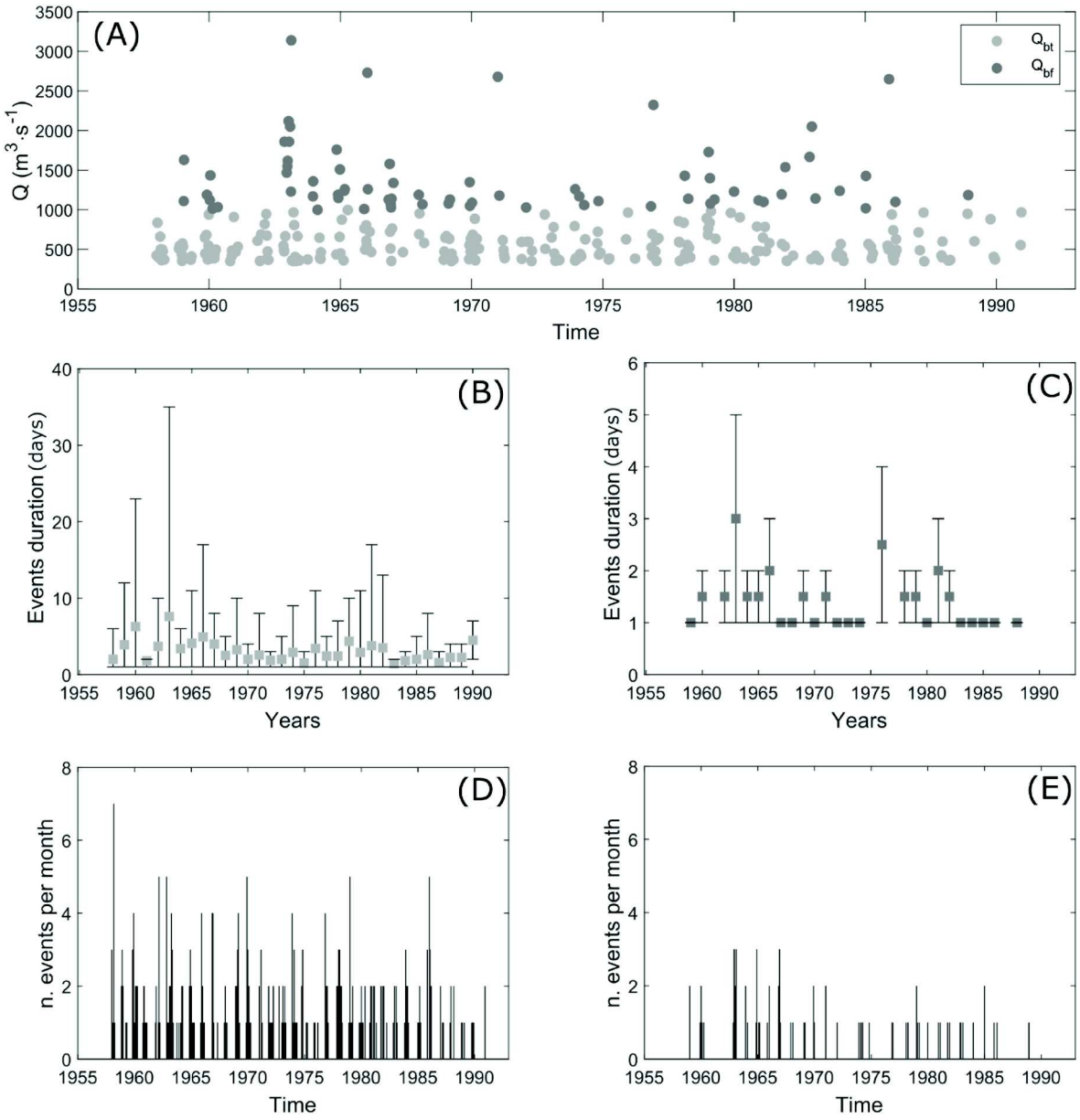

Fig. 4. Analysis of daily flow events above threshold recorded at Dorez station, in terms of their peak discharge (A), duration (B, C) and frequency (D, E; number of events per month). Streamflow thresholds: Q_{bt} = 350 m^3/s, initiation of bedload transport, and Q_{bf}, = 1000 m^3/s, bankfull discharge, respectively, light and dark grey). In B): duration above Q_{bt} and C): duration above Q_{bf}) square markers denote the yearly average value of events duration, while the upper and lower bars indicate the maximum and minimum values recorded in the same year. D) number of events above Q_{bt}, and E) number of events above Q_{bf}.

those emerging from ERA5 rainfall reanalysis on the catchment (Fig. 5). This suggests the opportunity to rely on the trend of rainfall reanalysis for the years in which historical streamflow data are not available (after 1990, and especially after 2000).

3.3. Analysis of human stressors

The analysis of forest land cover change (Fig. 6A) outlined a net forest loss of 739 km^2 from 1986 to 2020 (−21%, from 3534 km^2 in 1986 to 2795 km^2 in 2020. Most (63%) of the total forest loss is found in the mountain physiographic unit (467 km^2), other 33% in the hill physiographic unit (246 km^2), and the remaining 4% in the lowland physiographic unit, coherently with forest cover distribution, which is larger in the upper catchment (Fig. 6D). The analysis shows a reduction in the forest cover with an average annual loss of 0.217 km^2 (σ_{forest} = 0.151 km^2). Forest loss appeared more intense until 2000, with an average annual forest loss of 0.315 km^2 ($\sigma_{bef2000}$ = 0.172 km^2) and a peak value of 0.75 km^2in 1996. After 2000, the average annual forest loss is evaluated as 0.14 km^2 ($\sigma_{aft2000}$ = 0.066 km^2), with a minimum annual forest loss of 0.055 km^2in 2016.

Mapping of sediment mining activities from 2004 to 2020 reveals 22 sediment mining areas within the river channel, mainly concentrated in the lower reaches, specifically near the main road network in correspondence of Shushica T4 (n = 3), Selenizza V2 (n = 1), Kashist V3 (n = 7) and Mifol V4 (n = 7) reaches. Sediment mining areas can be observed also along the downstream part of the T3 reach of the Drinos tributary (n = 1) and in correspondence to Tepelene and Memaliaj settlements (n = 3, see Fig. 6A and B for sediment mining locations). The likelihood of sediment mining for 1968–2004 is derived by combining remote sensing and interviews with local stakeholders. Corona Images showed the absence of sediment mining activities in 1968 in detectable reaches. Apart from results derived from remote sensing, interviews with local

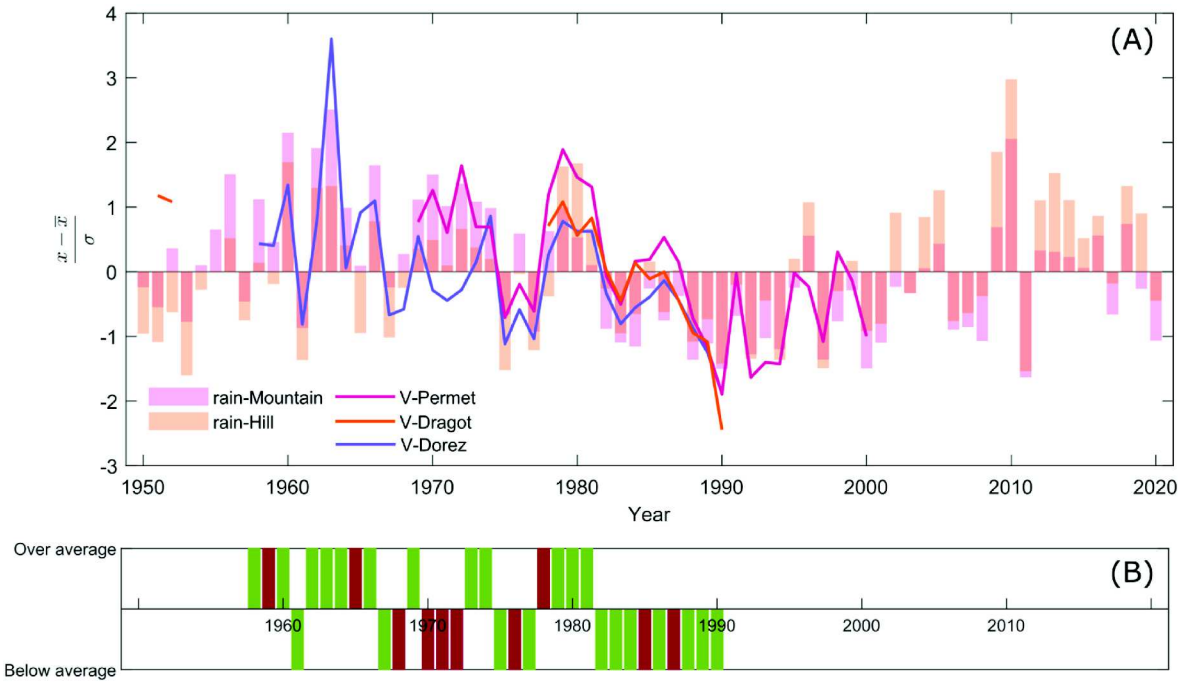

Fig. 5. Temporal analysis of annual streamflow volumes and rainfall time series. (A) Normalized rainfall values in the two physiographic units (pink: mountain; orange: hill) and normalized annual streamflow volumes. (B) Vertical bars indicating years with positive (green) and negative (red) correlations between rainfall-derived inflow trends and streamflow trends (from recorded discharges) at the Dorez station. Vertical bars above (below) the horizontal line represent events above (below) the average of the entire record. (For interpretation of the references to colour in this figure legend, the reader is referred to the Web version of this article.)

stakeholders also revealed the likely presence of sediment mining activities since the 1990s in the lower Shushica (T4), Kashisht V3, and Mifol V4 reaches (Fig. 6C).

Mapping of riverbanks erosion control works showed higher concentrations of bank protection and groynes structures in the lowland part of the river since 2004, where the floodplain hosts agricultural landscapes and villages subjected to flood risk (Fig. 6B and C). These bank protection structures reinforce most of the external banks, strongly limiting the river dynamicity. Corona Images showed the absence of riverbanks structure in 1968, with the exception of a series of groynes located near an active channel bend in the Kashisht V3 reach (Fig. 6C).

The impact of the Pigai Hydropower Plant on the river flow regime showed a statistically significant change point after dam building, considering both the seasonal and annual volume time series (further information in Fig. S11). The observed decreased annual volume at Permet station is caused by a decrease of the low flow, whereas the bankfull discharge is likely not affected, considering the small proportion of the catchment impounded by the dam. Moreover, such alteration is smoothed downstream due to the contribution of several tributaries. The most upstream reach we consider on the Vjosa main stem (V1) has a catchment area that is twice that of Permet station, suggesting the effect of the Pigai HPP to be negligible.

Finally, although the relevant seismic activity of the Balkan region may be a relevant driver for sediment supply, there is no evidence regarding seismic activity within the Vjosa river catchment influencing the river morphodynamics in the last 7 decades: no earthquakes with magnitude M $\geq$ 6 are reported within the catchment in the period 1950–2020 (U.S. Geological Survey, 2022).

3.4. Linkages between geomorphological processes, climatic and anthropic drivers

Linkages between geomorphological processes and climatic - anthropic drivers of change were identified separately for the three time periods that emerge from Section 3.1.1 (Table 3). The Mann Kendall trend test has been applied to hydrological pressure descriptors (streamflow time series, where available, and ERA5 rainfall) separately for each period to derive the directionality of hydrological pressures. Sediment mining emerges as the most relevant anthropic pressure for morphological change, given the likely low impact of land cover change, which is limited in rate and extent, and of river embankments, which are localized in smaller portions of the river, For the most recent period (2005–2020), the increasing intensity of sediment mining is evaluated by accounting for both in-channel local and upstream sediment mining sites for every reach. Table 3 indicates that, at the catchment scale, the morphological response is completely different between the oldest (1968–1985) and the most recent (2015–2020) time periods.

4. Discussion

Here we synthesize the main findings of the proposed approach and focus on discussing how the morphological trajectories of free-flowing rivers can be relevant to support their management, particularly because they allow the recognition of specific drivers of morphological change, which can be the target of management actions, by drawing on the results of the Vjosa river case study. We comment on the challenges of determining the morphological trajectories in data-scarce contexts, typical of many FFRs worldwide, and on possible coping strategies, such as those employed in our work. A synthesis of the limitations of the work and future research needs closes the section.

4.1. Catchment- and reach-scale morphological trajectories of the Vjosa river

A coherent morphological response can be observed in all selected reaches in the first (1968–1985) and second (1985–2000) time periods. Given the modest relevance of other stressors, hydrological variations appear to be the most influential driving factor for such change intense narrowing. The narrowing rate decreases in the subsequent periods, with several upstream reaches even reversing the trend. Such a decrease

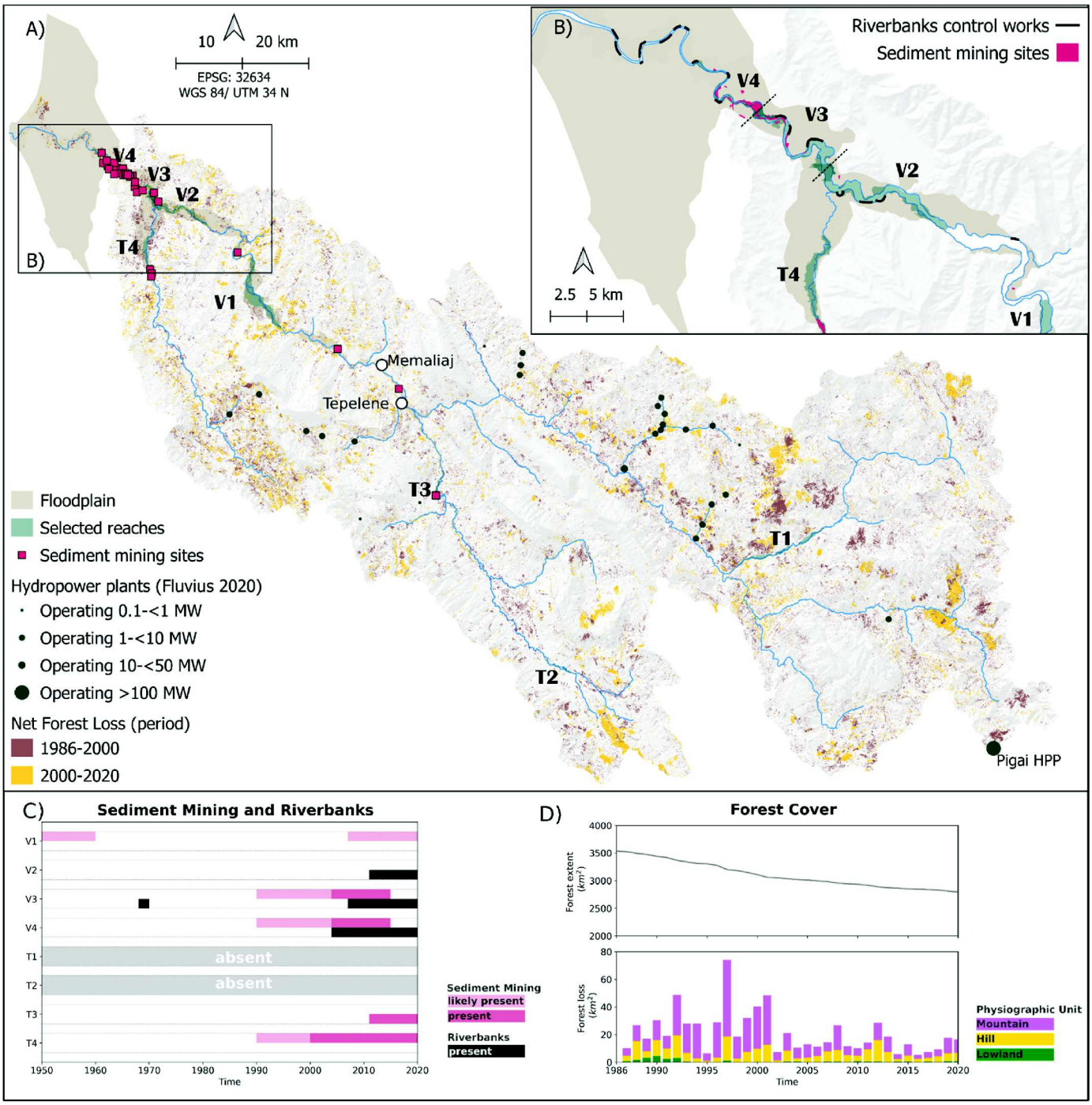

Fig. 6. Multiple human pressures maps on the Vjosa river catchment: (A) Forest land cover variation and relevant hydropower plants in the catchment; (B) sediment mining and bank control works in the lower segment; (C) persistence of sediment mining activities in the lower reaches; and (D) and Yearly forest loss in each physiographic unit.

of narrowing rates after the more intense and frequent floods in the 1960s can be interpreted as a morphological recovery during the following decades, characterized by a lower frequency and duration of formative events. Conversely, in the most recent period (2005–2020), narrowing is present only in the lowermost reaches V4 and T4, reflecting the occurrence of more intense human pressures, mainly localized in the lowest reaches. The other reaches, instead, show a mild widening trend, differently from what could be observed in the previous periods, in which all reaches showed a similar trend.

The headwater reaches (Sarandaporo T4 and Drinos upstream T2) are the most intact and natural of the system; showing analogous trajectories, essentially without human pressure. Here the narrowing rates decrease over time (from 35% to 24%–1%), which can therefore be interpreted as a morphological response to the solely climatic driver, specifically the decrease in duration, frequency and magnitude of geomorphic relevant floods with respect to the 1960s, with the present configuration being in equilibrium with the new flow regime. Taking into account all the selected reaches, the system presents narrowing rates from 73% to 29%, with an average narrowing of 47% from 1968 to 2020.

Considering the significant decreasing trends observed in flood frequency and duration, and in flood magnitude (though not significant)

Table 3
Catchment-scale outlook of reach-scale variations of the active width and related pressures in the three considered time periods. Symbols: ↓ Narrowing trend; ↓↓ intense narrowing; ↑ widening trend; ↑↑ intense widening; - Absent/no trend; ↑^: widening likely present (estimated). n.a.: no data available, A double asterisk (**) in the last time period indicates that the channel morphology type of the reach has changed (Section 3.1.2). The use of one or two arrows has to be viewed in a semi-quantitative way, as the intensity of the narrowing is comparable only within the same river reach (vertical reading of the table), reflecting the information reported in the lower panel of Fig. 3A.

Period 1 - 1968–1985								
River reaches	V1	V2	V3	V4	T1	T2	T3	T4
Morphological response*	↓↓	↓↓	↓↓	↓↓	n.a.	↓↓	n.a.	↓↓
Hydrological pressure	↓	↓	↓	↓	↓	↓	↓	↓
Anthropic pressure	↑^	–	–	–	–	–	–	–
Period 2 - 1985–2000								
River reaches	V1	V2	V3	V4	T1	T2	T3	T4
Morphological response*	↓	↓	↓	↓	↓	↓	↓	–
Hydrological pressure	–	–	–	–	–	–	–	–
Anthropic pressure	–	↑^	↑^	↑^	–	–	–	↑^
Period 3 - 2005–2020								
River reaches	V1	V2	V3	V4	T1	T2	T3	T4
Morphological response*	–	↑**	↑	↓**	–	–	–	↓
Hydrological pressure	–	–	–	–	–	–	–	–
Anthropic pressure	–	↑	↑	↑	–	–	–	↑↑

after the 50-year flood in 1963, our results suggest that the observed catchment-scale narrowing, which occurred at progressively lower rates, can reflect a "relaxation phase" of the system (e.g., Peters et al., 2021; Milan, 2012). Such relaxation started after the channel widening that could not be detected in this analysis, but which likely occurred in the early 1960s, associated with a flood-intense period. Relaxation was then probably already underway in 1968 (Fig. 3B), and the observed progressive reduction in narrowing rates suggests that reaches with minimal anthropic effects may now be close to "regime conditions" at equilibrium with the present, less dynamic flow regime (Fig. 5).

The lower reaches of the selected Vjosa tributaries (Drinos downstream T3 and Shushica T4) appear to have been affected by sediment mining activities in the last 5 and 15 years, respectively. While Drinos downstream T3 reach does not display a clear narrowing trend, Shushica T4 shows a clear narrowing response and warns of a possible analogous response of T3 soon. Indeed, sediment mining has an immediate widening effect due to vegetation removal and reduction of riverbed cohesion, while in the longer term, it produces channel incision and subsequent active channel narrowing (Kondolf, 1997), as in the lower Shushica river. The Kuta V1 reach shows a 30% narrowing with a constant trend over the entire period of analysis. Finally, reaches of the lowland Vjosa's main course (V2, V3, V4) present a progressive geomorphic relaxation after the flood intense period, passing from a clear narrowing phase in 1968–2000 to a more recent widening trajectory (2000–2020) (Table 3).

Overall, the analysis of this case study reveals the importance of both a catchment-scale view of controlling factors and a further focus on a reach-scale view to capture and interpret the distinct response patterns that have occurred in the system, especially in relation to the most pronounced and spatially concentrated human effects. Our observations of the system response to sediment mining are consistent with Surian et al. (2009), suggesting a time lag of almost a decade between pressure and response, as observed during the 1980–1990 decade in France, Italy, Poland and Romania (Zawiejska and Wyżga, 2010; Armaş et al., 2013; Rădoane et al., 2013; Surian, 2022).

The analysis also shows that the role of sediment mining as a stressor on FFRs may have been so far underrated. Indeed FFRs have been characterized so far mainly through their longitudinal hydrological connectivity, which is normally quantified with indicators that are not affected by the presence of sediment mining in the active river channel. The relevance of unsustainable sediment mining has also been shown for other large rivers (Schmitt et al., 2018). In the last decade, reported threats to the conservation of Balkan FFRs have been mainly focusing on hydropower development (Zarfl et al., 2019; Carolli et al., 2023); however, our study highlights the importance to account for sediment mining as a key source of hydromorphological alteration especially in the lowland reaches, which may even result in a complete change of the channel pattern (as V4 reach in the Vjosa case study), heavily affecting the ecological integrity.

4.2. Morphological trajectories and their relevance for the management of FFRs

So far, almost no study addressed the relevance of morphological trajectories for FFRs management despite their relevance at multiple levels: (a) for preserving habitat and ecosystem integrity; (b) for flood risk management; and (c) for zonation at a legal level when FFRs are part of natural protected areas, like in the case of the Vjosa Wild River National Park.

First, morphological trajectories define the historical variations of the active river corridor, which allow to set objective boundaries for the occurrence of processes of floodplain retreat and advance. In Europe and in general in contexts with diffuse river regulation, river recovery towards an improved hydro-morphological condition is increasingly relevant among management agencies interested in conservation of the natural capital (Fryirs and Brierley, 2016). To address the potential of river recovery requires reconstructing past and present trajectories of adjustment, through a scenario-building approach (Ziliani and Surian, 2012). In the case of FFRs, this can provide a process-based criterion to set minimum management boundaries for the fluvial landscape. In the case of the Vjosa, the borders of the active river corridor may be used to define the boundaries of the National Park, or they can serve as an operational reference to define the internal zonation of the protected area.

Moreover, morphological trajectories support the identification of different eco-morphological behaviors of river reaches. Any modification of the morphology of a river reach potentially leads to an alteration of its ecological communities. The case study of the Vjosa shows that reaches may be subject to relevant changes even in an FFR. For example, Selenizza V2 and Shushica T4 reaches have transitioned from a wandering to a sinuous and from a braided to a wandering morphology, respectively (Fig. 3B–Table 3) because of the combined effect of climate variability and sediment mining. As indicated in Belletti et al. (2017) the abundance and diversity of habitat types (geomorphic units, or meso-habitats) varies for different river morphologies. Therefore, morphology simplification and shift from multi-thread to single threads significantly decrease the original heterogeneity and richness of habitat types, and can therefore imply strong changes in habitat availability and ecosystem services. From a management viewpoint, this can support decision-making about the upstream regulation of the flow and sediment supply regimes (e.g., water abstractions sites, reservoirs, sediment mining sites, authorizations etc.), because these regimes are the primary drivers of the channel adjustments (e.g. Rinaldi et al., 2015). Furthermore, the lateral dynamics of the active corridor allow to account for the lateral connectivity alteration (Shen and Liu, 2021), which has been scarcely integrated into management frameworks, so far.

The boundaries of the active river corridor also define lower limits of historical inundation extents, and therefore lower limits of potential future flooded areas. For example, reach Kuta V1 had a vast portion of the present floodplain included in the active corridor until the late 1980s (Fig. S1). Also, Shushica T4 shows 50% of the active corridor in 1968 becoming floodplain in recent years (Fig. 3B). While so far these areas tend to be occupied mainly by agricultural activities in the case of the Vjosa, in many other contexts such areas are planned as more intensively anthropized, heavily increasing the hazard for human communities. Knowledge of the size and location of these areas is therefore useful to support strategies for flood risk management, especially in data-scarce

contexts, where accurate hydrological data and flood inundation information are often hardly available.

Given the recent establishment of the Vjosa river National Park, this work supports the development of management and regulatory framework for the first designated wild river area in Europe, not only focusing on the longitudinal connectivity of the river but also integrating further important parameters that are strongly related to its overall ecological condition.

4.3. Isolating the geomorphic effects of climatic oscillations and major flood disturbances in FFRs

The work allowed isolating the role of climatic oscillations and related major flood disturbance events on river morphological changes. This is an example of a rather unique research opportunity provided by FFRs. For reaches in which the role of other anthropogenic stressors can be considered negligible, the observed temporal changes can be viewed as the 'natural' variability of the system driven by the changes in the flow regime.

The detected variability of the streamflow series is coherent with climatic and hydrological trends of the past 4 to 5 decades in the Mediterranean region when Balkan rivers have undergone relevant discharge reduction (Skoulikidis et al., 2022). Severe drought at the end of the 1980s - early 1990s followed a period of intense hydrological activities in the 1960s, with a significant reduction of the annual discharge of the Vjosa river from 1964 to 1987 (−24% in Greece and −19% in Albania) (Skoulikidis et al., 2022). From our results, the Vjosa system's active width appears to be importantly influenced by medium to large floods (Q_{bf}), which decreased in frequency and duration from 1958 to the 1990s, but most likely also by the 50-year flood in 1963, which occurred in a hydrologically intense period. Which main driver has set the larger active channel widths measured immediately after that period (1968 images, Fig. 3B) - the largest flood event, or multiple flood events of different magnitudes in the same wet period - is difficult to assess. The few available literature on climatic effects on channel adjustments suggests that the two types of drivers (largest flood vs. hydrologically intense period) could somehow act separately.

Grams et al. (2020) pointed out that a decrease in peak-flow magnitude and duration (either naturally or anthropogenically driven) likely leads to channel narrowing in the Green River in Canyonlands National Park, Utah. Moreover, moderate to large floods, combined with reduced time intervals between mean annual floods, represented primary controls on floodplain width and erosion of vegetated areas, in the Sarine River, Switzerland (Tonolla et al., 2021). Batalla et al. (2018) describe how the reduction of formative discharges due to the recent low hydroclimatic activity appears to be the main control on the evolution of the wandering River Ñuble, in the Mediterranean climate region of Chile. As for human-impacted systems, Belletti et al. (2015) showed the major relevance of the recent flood history in influencing the width patterns and vegetation responses of 53 braided reaches in the Rhone watershed, France, compared to other regional and local factors. The role of climatic versus anthropogenic factors has also been demonstrated for Romanian rivers (Rădoane et al., 2013). There are almost no cases worldwide where monitoring programs have provided an adequate database to quantify geomorphic responses to major disturbance events on multidecadal timescales (Tunnicliffe et al., 2018). In these terms, the detected system relaxation (Knighton, 1998) after a major catchment disturbance in the Vjosa represents an important addition to the few cases reported in the literature and a baseline that should be integrated into the hydromorphological components of the management plans that are presently under development. Our results can be viewed in the perspective of the river sensitivity concept (Fryirs, 2016) at the reach scale, specifically in terms of the active channel adjustment rate and magnitude with a five-year observation resolution. On the temporal dimension, we describe the system relaxation to climatic variations and some relevant localized responses due to sediment mining and channelization. Moreover, our results warn about the impact of sediment mining activities on the evolutionary trajectory because they alter the system's inherent sensitivity. Milestone principles to assess river sensitivity have been discussed for decades, and nowadays the key challenge is to apply the concept and assess river sensitivity across spatial and temporal scales (Brunsden and Thornes, 1979; Allison and Thomas, 1993; Fryirs, 2016), taking advantage of more mature and powerful tools. Multispectral satellite imagery is increasingly used to reveal fluvial dynamics in large rivers (Henshaw et al., 2013, Monegaglia et al., 2018; Spada et al., 2018; Boothroyd et al., 2020; Harezlak et al., 2020), thus overcoming previous limitations especially by offering increasing resolution potential (in time and space) for the assessment of river sensitivity in relation to channel morphodynamics. The baseline knowledge on the morphological sensitivity and recovery time developed in this work set the basis for future studies for the investigation of the Vjosa river geomorphic sensitivity. For example, the detected river sensitivity to streamflow variations suggests an extreme caution in terms of licensing future water (and sediment) abstractions, impoundments and dams on the Vjosa main river stem and on its largest tributaries. Further research is suggested to understand the morphological adjustment rates to relevant flow and sediment regulations that might have dramatic effects in terms of reduced habitat availability for most of the unique and rare species that characterize this free-flowing river system (Schiemer et al., 2020). Several studies have shown that several multi-thread, braided rivers across the globe have already dramatically changed their channel morphology by shifting towards single-thread channel patterns due to sediment undernourishment, construction of flood protection works and river flow regulation by dams over the last century (Bizzi et al., 2019; Stecca et al., 2019; Kondolf, 1997; Surian and Rinaldi, 2003). Analogous evolutions have been already detected in the sensitive Shushica T4 and Selenizza V2 lowland reaches of the Vjosa river system. Also the recent modeling study of Bizzi et al. (2021) suggested that the present conditions of several multi-thread reaches in the Vjosa are such that small perturbations of their flow and sediment supply regimes can determine transitioning to single-thread patterns, which further supports this dynamic river to be characterized by a high geomorphic sensitivity.

4.4. Challenges posed by data-scarcity, coping strategies and limitations of the work

Considering the current fragmentation and paucity of information on river hydromorphology and human impacts on large free-flowing rivers worldwide, including the Vjosa river corridor, our results show how in data-scarce contexts, the combination of different approaches (remote sensing, socio-cultural indicators, combination of hydrometric and rainfall data, among others) allows the detection of river evolutionary trajectories and related indicators, which can be interpreted in the light of context-specific semi-quantitative information on human pressures. The increasing availability of satellite imagery at a global scale provides a valuable data source to reconstruct the morphological evolution of FFRs, which are often located in remote areas (Betz et al., 2020).

To this purpose, Corona's declassified images represent a valid source of information to get the state of rivers decades before the advent of Landsat missions. The nearly global coverage and the high resolution of such products make it possible to get a solid reference of active river's corridor width and morphology in the 1960s and 70s, a precious data source, for instance, in the study of climate change effects on river morphology.

One of the main limitations of the employed approach is related to the relatively coarse spatial resolution of Landsat imagery, which is the most commonly open-access source and is one of the few going back 4 decades. In our case, the 30 m spatial resolution of Landsat imagery determined an error in the range of 3%–8% for the majority of the reaches. The only exception is the Drinos upstream reach, which can be considered as a limit for the applicability of this remote sensing

procedure, due to its smaller width (150 m). The integration of super-resolution mapping (SRM) algorithms is promising to increase the accuracy of channel active width quantification in the proposed cloud-based remote sensing analysis of river morphodynamics, as pointed out by Niroumand-Jadidi and Vitti (2017), who showed an improved accuracy of about 10% compared to the conventional hard classification. Moreover, Carbonneau et al. (2020) developed a convolutional neural network classifier, trained using UAV imagery, which mapped water, sediment and vegetation classes with an accuracy greater than 95%.

Similarly, the significance of Google Earth-derived indicators for mapping sediment mining and bank protection works depends on the number, timing, and resolution of images available in the database for each reach. While hydro-morpho-ecological indicators extracted from Google Earth are clearly affected by the lack of control over flow stage and/or season at the time of image acquisition (Henshaw et al., 2019), in the present work, the procedure used to map human interventions along the river corridor is independent of seasonality. Accurate temporal quantification of human pressures is hampered in our case by the small number of useable Google Earth images related to our reaches, which nevertheless allow the extraction of relevant qualitative information.

Also retrieving qualitative socio-cultural information can support the reconstruction of anthropogenic effects in data-scarce contexts. For example, qualitative information about likely sediment mining activities along the river corridor has proven to be relevant to understanding past pressures near the settlements of Memaliaj and Tepelene (Fig. 1). Indeed, the construction of the Memaliaj village dates back to 1947, to host workers of the nearby mining areas. As the road network has only been expanded in the last 5 years, the village may likely have been built using the sediments from the Vjosa river, as the unique cheap local source of building materials. No official data on gravel mining and river reinforcements before 2004 is available. To the authors' knowledge, until the beginning of the 1990s, the totalitarian regime strictly managed all activities and infrastructure in the country. Any intervention or abstraction from the river was state-controlled. New constructions and internal displacements were very limited at that time. In the 1990s, after the fall of the regime, there was an uncontrolled opening to the market, while the legislative framework was particularly weak and poorly enforced about landscape and urban planning. This caused increasing human pressure on the environment, and particularly on river sediments to support rapid urban and infrastructural expansion.

Despite forest harvesting occurring at modest rates in several areas close to villages and settlements, agricultural abandonment and rural-to-urban and international migration appear to be consistent with the absence of clear-cutting and massive deforestation activities within the Vjosa watershed, which might have represented an important driver of channel adjustment through its potential effect on sediment supply. Furthermore, Mediterranean climatic conditions do not support the colonization of floodplains and abandoned fields by mature forests, analogous to what is observed in southern Italy, which has an analogous climate (Scorpio and Piègay, 2021). However, further studies are needed to understand the complex site-specific mechanisms of bio-geomorphic interactions within the river corridor. Considering our results at the catchment scale, we detected a gradual and rather limited reduction in forest cover, especially in the mountain areas (more than 45 river km upstream of the V2 reach) and before 2000. This suggests that forest loss is unlikely to have played a relevant role in the recent channel widening observed in the lowland reaches.

Limitations in the availability of streamflow data constrained the present study and emphasized the importance of improving regular monitoring of river flow and channel morphology and making data available for research and management purposes, an important hurdle for river management in the area. The combined use of ERA5 cumulative rainfall data and available hydrometric data has nevertheless proven to be a valuable opportunity to improve the semi-quantitative description of streamflow variability and of possible climatic trends over time. Aggregate statistics are preferable to point data for such analysis. In this work, we preferred to use annual and monthly aggregations of daily rainfall and streamflow data to filter out plausible uncertainties. Sub-catchment area ratios and distance to ERA5 centroids were also taken into account to compare the time series of cumulative rainfall and monthly and annual flows.

5. Conclusions

The present work aimed to demonstrate the importance of broadening the characterization of FFRs, beyond their longitudinal connectivity alone, by including indicators related to their processes of morphodynamic evolution on a multi-decadal time scale, which are key for their sustainable management. Specifically, the work has increased the understanding of the morphological evolution of large, free-flowing river corridors in a temperate Mediterranean climate, and their relationship with possible drivers of change, and showed how to address its data-scarce context. We proposed an innovative, multi-scale and multi-temporal form- and dynamics-based approach to the study of river evolutionary trajectories, mostly using freely available data sources such as Landsat imagery and ERA5 precipitation reanalysis.

The approach was applied to the case study of the free-flowing Vjosa river and three of its tributaries in Albania over 50 years (1968–2020). Our analysis reveals that climate-related change in the flood regime is the leading driver for decadal morphological adjustment at the catchment scale, an effect that has been seldom observed in previous studies, and which can be specifically appreciated mainly in FFRs. The Vjosa river system appears to be recovering from the 1960s flood-intense period and is now facing a different hydrological regime characterized by a decreased frequency and duration of formative events. The system shows an average catchment-scale river corridor narrowing of 47%, at rates that decreased over the last 5 decades from 35% narrowing (1968–1985) to 24% narrowing (1985–2000), to no catchment scale change (1% narrowing from 2005 to 2020).

Although the Vjosa is considered a free-flowing river system of European significance, our analysis highlights the presence of anthropic pressures that are mostly concentrated in its lower catchment and that occurred mainly in the last 2 decades, after marked social and political changes in the country. At local scale, sediment mining has likely contributed to a 30% reduction of the active width, significantly impacting the evolutionary trajectory and the ecological condition of lowland reaches. Recognizing such specific spatial and temporal dimensions of human effects, further supports our conclusion on the major role of climate variability in the less human-impacted reaches, which are the majority in the system.

The work ultimately shows how the incorporation of the morphological trajectories and of their drivers in the characterization of FFRs represents a key baseline knowledge in terms of habitat conservation, flood risk management and physically-based criteria for the definition of legal boundaries and zonation of protected areas centered on the FFRs, through the example of the Vjosa Wild River National Park.

CRediT authorship contribution statement

Marta Crivellaro: Writing – original draft, Visualization, Software, Methodology, Formal analysis, Data curation, Conceptualization. **Livia Serrao:** Writing – original draft, Visualization, Software, Methodology, Formal analysis, Data curation, Conceptualization. **Walter Bertoldi:** Writing – original draft, Visualization, Supervision, Methodology, Formal analysis, Data curation, Conceptualization. **Simone Bizzi:** Writing – original draft, Conceptualization. **Alfonso Vitti:** Supervision, Methodology. **Christoph Hauer:** Writing – original draft. **Klodian Skrame:** Data curation. **Bestar Cekrezi:** Data curation. **Guido Zolezzi:** Writing – original draft, Supervision, Project administration, Funding acquisition, Formal analysis, Data curation, Conceptualization.

Declaration of competing interest

The authors declare the following financial interests/personal relationships which may be considered as potential competing interests: Marta Crivellaro reports financial support was provided by Volontariato Internazionale per lo Sviluppo VIS and CESVI. If there are other authors, they declare that they have no known competing financial interests or personal relationships that could have appeared to influence the work reported in this paper.

Data availability

Data will be made available on request.

Acknowledgments

Authors thank the two anonymous reviewers whose suggestions helped improve and clarify this manuscript. This work was realized in the framework of the activities of the UNESCO Chair in Engineering for Human and Sustainable Development of the University of Trento. Financial support has been provided by VIS (Volontariato Internazionale per lo Sviluppo) and CESVI Onlus within "GREEN coAL-ITion: Eco-sustainable Development for Albanian mountain-countryside natural capital" project [Lot1: CIG 81366342CA]. It has also been supported by the Italian Ministry of Universities and Research (MUR), in the framework of the project DICAM-EXC (Departments of Excellence 2023–2027, grant L232/2016); Guido Zolezzi acknowledges the support by the European Union under NextGeneration EU. PRIN 2022 "SEDMORNET" Prot. n. E53D23004200006.

Appendix A. Supplementary data

Supplementary data to this article can be found online at https://doi.org/10.1016/j.jenvman.2024.122541.

References

Albert, J.S., Destouni, G., Duke-Sylvester, S.M., Magurran, A.E., Oberdorff, T., Reis, R.E., Winemiller, K.O., Ripple, W.J., 2020. Scientists' warning to humanity on the freshwater biodiversity crisis. Ambio 50 (1), 85–94.

Allison, R.J., Thomas, D.S.G., 1993. The sensitivity of landscapes. In: Thomas, D.S.G., Allison, R.J. (Eds.), Landscape Sensitivity. John Wiley & Sons, Chichester, pp. 1–5.

Armaş, I., Gogoaşe Nistoran, D.E., Osaci-Costache, G., Braşoveanu, L., 2013. Morpho-dynamic evolution patterns of subcarpathian Prahova river (Romania). Catena 100, 83–99.

Arnaud, F., Schmitt, L., Johnstone, K., Rollet, A.J., Piégay, H., 2019. Engineering impacts on the Upper Rhine channel and floodplain over two centuries. Geomorphology 330, 13–27.

Auerbach, D.A., Deisenroth, D.B., McShane, R.R., McCluney, K.E., Poff, N.L., 2014. Beyond the concrete: accounting for ecosystem services from free-flowing rivers. Ecosyst. Serv. 10, 1–5.

Bartłomiej Wyżga, 20 A review on channel incision in the Polish Carpathian rivers during the 20th century, Editor(s): Helmut Habersack, Hervé Piégay, Massimo Rinaldi, Developments in Earth Surface Processes, Elsevier, Volume 11, 2007, Pages 525-553, ISSN 0928-2025, ISBN 9780444528612.

Batalla, R., Iroumé, A., Hernández, M., Llena, M., Mazzorana, B., Vericat, D., 2018. Recent geomorphological evolution of a natural river channel in a Mediterranean Chilean basin. Geomorphology 303, 322–337.

Beechie, T.J., Sear, D.A., Olden, J.D., Pess, G.R., Buffington, J.M., Moir, H., Roni, P., Pollock, M.M., 2010. Process-based principles for restoring river ecosystems. Bioscience 60, 209–222.

Bell, B., Hersbach, H., Simmons, A., Berrisford, P., Dahlgren, P., Horányi, A., et al., 2021. The ERA5 global reanalysis: preliminary extension to 1950. Q. J. R. Meteorol. Soc. 147 (741), 4186–4227.

Belletti, B., Dufour, S., Piégay, H., 2015. What is the relative effect of space and time to explain the braided river width and island patterns at a regional scale? River Res. Appl. 31, 1–15.

Belletti, B., Rinaldi, M., Bussettini, M., Comiti, F., Gurnell, A.M., Mao, L., Nardi, L., Vezza, P., 2017. Characterising physical habitats and fluvial hydromorphology: a new system for the survey and classification of river geomorphic units. Geomorphology 283, 143–157.

Belletti, B., de Leaniz, C.G., Jones, J., Bizzi, S., Börger, L., Segura, G., Castelletti, A., Van de Bund, W., Aarestrup, K., Barry, J., Belka, K., Zalewski, M., 2020. More than one million barriers fragment Europe's rivers. Nature 588 (7838), 436–441.

Best, J., 2019. Anthropogenic stresses on the world's big rivers. Nat. Geosci. 12 (1), 7–21.

Betz, F., Lauermann, M., Cyffka, B., 2020. Open source riverscapes: analyzing the corridor of the Naryn River in Kyrgyzstan based on open access data. Rem. Sens. 12 (16), 2533.

Bizzi, S., Demarchi, L., Grabowski, R.C., Weissteiner, C.J., van de Bund, W., 2015. The use of remote sensing to characterize hydromorphological properties of European rivers. Aquat. Sci. 78 (1), 57–70.

Bizzi, S., Piégay, H., Demarchi, L., de Bund, W.V., Weissteiner, C.J., Gob, F., 2019. LiDAR-based fluvial remote sensing to assess 50–100-year human-driven channel changes at a regional level: the case of the Piedmont Region, Italy. Earth Surf. Process. Landforms 44 (2), 471–489.

Bizzi, S., Tangi, M., Schmitt, R.J.P., Pitlick, J., Piégay, H., Castelletti, A.F., 2021. Sediment transport at the network scale and its link to channel morphology in the braided Vjosa River system. Earth Surf. Process. Landforms 46 (14), 2946–2962.

Boothroyd, R.J., Williams, R.D., Hoey, T.B., Barrett, B., Prasojo, O.A., 2020. Applications of Google Earth Engine in fluvial geomorphology for detecting river channel change. WIREs Water 8, 1.

Boothroyd, R.J., Nones, M., Guerrero, M., 2021a. Deriving planform morphology and vegetation coverage from remote sensing to support river management applications. Front. Environ. Sci. 9.

Boothroyd, R.J., Williams, R.D., Hoey, T.B., Tolentino, P.L., Yang, X., 2021b. National-scale assessment of decadal river migration at critical bridge infrastructure in the Philippines. Sci. Total Environ. 768, 144460.

Brasseur, M.V., Martini, J., Wilfling, O., Wüthrich, R., Birnstiel, E., Oester, R., et al., 2023. Exploring macroinvertebrate biodiversity in the dynamic southern Balkan stream network of the Vjosa using preservative-based DNA metabarcoding. Aquat. Sci. 85 (2), 51.

Brierley, G.J., Fryirs, K.A., 2005. Geomorphology and River Management: Applications of the River Style Framework. Blackwell, Oxford, U.K.

Brierley, G.J., Fryirs, K.A., 2016. The use of evolutionary trajectories to guide 'moving targets' in the management of river futures. River Res. Appl. 32, 823–835.

Brierley, G.J., Fryirs, K.A., Outhet, D., Massey, C., 2002. Application of the river styles framework as a basis for river management in New South Wales, Australia. Appl. Geogr. 22, 91–122.

Brunsden, D., Thornes, J.B., 1979. Landscape sensitivity and change. Trans. Inst. Br. Geogr. 4 (4), 463–484.

Carbonneau, P.E., Piegay, H., 2012. Fluvial Remote Sensing for Science and Management. Wiley, Chichester.

Carbonneau, P.E., Belletti, B., Micotti, M., Lastoria, B., Casaioli, M., Mariani, S., Marchetti, G., Bizzi, S., 2020. UAV-based training for fully fuzzy classification of Sentinel-2 fluvial scenes. Earth Surf. Process. Landforms 45 (13), 3120–3140.

Carolli, M., Garcia de Leaniz, C., Jones, J., Belletti, B., Huđek, H., Pusch, M., Pandakov, P., Börger, L., van de Bund, W., 2023. Impacts of existing and planned hydropower dams on river fragmentation in the Balkan Region. Sci. Total Environ. 871, 161940.

Comiti, F., 2012. How natural are Alpine mountain rivers? Evidence from the Italian Alps. Earth Surf. Process. Landforms 37 (7), 693–707.

Comiti, F., Da Canal, M., Surian, N., Mao, L., Picco, L., Lenzi, M.A., 2011. Channel adjustments and vegetation cover dynamics in a large gravel-bed river over the last 200 years. Geomorphology 125 (1), 147–159.

Coulthard, T.J., Van de Wiel, M.J., 2013. Climate, tectonics or morphology: what signals can we see in drainage basin sediment yields? Earth Surf. Dyn. 1 (1), 13–27.

Crivellaro, M, Vitti, A, Zolezzi, G, Bertoldi, W, 2024. Characterization of Active Riverbed Spatiotemporal Dynamics through the Definition of a Framework for Remote Sensing Procedures. Remote Sensing 16 (1), 184. https://doi.org/10.3390/rs16010184.

Eco-Masterplan for Balkan rivers, 2018. "Save the Blue Heart of Europe" Campaign.

EuroNatur, Riverwatch, FLUVIUS (2012-2020). Balkan Rivers – the Blue Heart of Europe, Hydromorphological Status and Dam Projects, Report. Vienna, March 2012 & Data Update 2020.

European Commission, Directorate-General for Environment, 2022. Nature Restoration Law – for People, Climate, and Planet. Publications Office of the European Union.

Fryirs, K.A., 2016. River sensitivity: a lost foundation concept in fluvial geomorphology. Earth Surf. Process. Landforms 42 (1), 55–70.

Fryirs, K.A., Brierley, G.J., 2016. Assessing the geomorphic recovery potential of rivers: forecasting future trajectories of adjustment for use in management. WIREs Water 3 (5), 727–748.

Geological Survey, U.S., 2022. Earthquake. accessed on 3th october 2022 at URL. https://earthquake.usgs.gov/.

Grabowski, R.C., Surian, N., Gurnell, A.M., 2014. Characterizing geomorphological change to support sustainable river restoration and management. WIREs Water 1, 483–512.

Graf, W., Pauls, S.U., Vitecek, S., 2018. Isoperla vjosae sp. n., a new species of the Isoperla tripartita group from Albania (Plecoptera: Perlodidae). Zootaxa 4370 (2).

Grams, P.E., Dean, D.J., Walker, A.E., Kasprak, A., Schmidt, J.C., 2020. The roles of flood magnitude and duration in controlling channel width and complexity on the Green River in Canyonlands, Utah, USA. Geomorphology 371, 107438.

Grill, G., Lehner, B., Thieme, M., et al., 2019. Mapping the world's free-flowing rivers. Nature 569 (7755), 215–221.

Gurnell, A.M., Bertoldi, W., Corenblit, D., 2012. Changing River channels: the roles of hydrological processes, plants and pioneer fluvial landforms in humid temperate, mixed load, gravel bed rivers. Earth Sci. Rev. 111 (1–2), 129–141.

Gurnell, A.M., Bertoldi, W., Tockner, K., Wharton, G., Zolezzi, G., 2016. How large is a river? Conceptualizing river landscape signatures and envelopes in four dimensions. Wiley Interdisciplinary Reviews: Water 3 (3), 313–325.

Harezlak, V., Geerling, G.W., Rogers, C.K., Penning, W.E., Augustijn, D.C.M., Hulscher, S. J.M.H., 2020. Revealing 35 years of landcover dynamics in floodplains of trained lowland rivers using satellite data. River Res. Appl. 36 (7), 1213–1221.

Hauer, C., Aigner, H., Fuhrmann, M., Holzapfel, P., Rindler, R., Pessenlehner, S., Pucher, D., Skrame, K., Liedermann, M., 2019. Measuring of Sediment Transport and Morphodynamics at the Vjosa River/Albania, vol. 85.
Hauer, C., Skrame, K., Fuhrmann, M., 2021. Hydromorphologial assessment of the Vjosa river at the catchment scale linking glacial history and fluvial processes. Catena 207, 105598.
He, F., Thieme, M., Zarfl, C., Grill, G., Lehner, B., Hogan, Z., Tockner, K., Jähnig, S.C., 2021. Impacts of loss of free-flowing rivers on global freshwater megafauna. Biol. Conserv. 263, 109–335.
Henshaw, A.J., Gurnell, A.M., Bertoldi, W., Drake, N.A., 2013. An assessment of the degree to which Landsat TM data can support the assessment of fluvial dynamics, as revealed by changes in vegetation extent and channel position, along a large river. Geomorphology 202, 74–85.
Henshaw, A.J., Sekarsari, P.W., Zolezzi, G., Gurnell, A.M., 2019. Google Earth as a data source for investigating river forms and processes: discriminating river types using form-based process indicators. Earth Surf. Process. Landforms 45 (2), 331–344.
Hersbach, H., Bell, B., Berrisford, P., Biavati, G., Horányi, A., Muñoz Sabater, J., Nicolas, J., Peubey, C., Radu, R., Rozum, I., Schepers, D., Simmons, A., Soci, C., Dee, D., Thépaut, J.-N., 2018. ERA5 hourly data on single levels from 1979 to present. Copernicus Climate Change Service (C3S) Climate Data Store (CDS), 14-APR-2021.
Hohensinner, S., Hauer, C., Muhar, S., 2018. River morphology, channelization, and habitat restoration. In: Riverine Ecosystem Management. Springer International Publishing, pp. 41–65.
Jézéquel, C., Oberdorff, T., Tedesco, P.A., Schmitt, L., 2022. Geomorphological diversity of rivers in the Amazon basin. Geomorphology 400, 108078.
Karen McVeigh, 2023. Historic moment' for nature as Europe's first wild river national park announced in Albania. Guardian. https://www.theguardian.com/environment/2023/mar/15/albania-vjosa-wild-river-national-park-europe-first-aoe. (Accessed 15 May 2023).
Kennedy, R.E., Yang, Z., Cohen, W.B., 2010. Detecting trends in forest disturbance and recovery using yearly Landsat time series: 1. Landtrendr—temporal segmentation algorithms. Remote Sens. Environ. 114, 2897–2910.
Kiss, T., Blanka, V., 2012. River channel response to climate- and human-induced hydrological changes: case study on the meandering Hernád River, Hungary. Geomorphology 175–176, 115–125.
Knighton, A.D., 1998. Fluvial Forms and Processes: A New Perspective. Arnold, London, p. 383.
Kondolf, G., 1997. PROFILE: hungry water: effects of dams and gravel mining on river channels. Environ. Manag. 21 (4), 533–551.
Kondolf, M., Zolezzi, G., 2008. Reference river ecosystems: historical states, best ecological potential and management challenges. Workshop summary. In: Proceedings of the IV European Congress on River Restoration, pp. 1059–1063. Venice, 2008.
Lach, J., Wyżga, B., 2002. Channel incision and flow increase of the upper Wisłoka River, southern Poland, subsequent to the reafforestation of its catchment. Earth Surf. Process. Landforms 27 (4), 445–462.
Liébault, F., Piégay, H., 2002. Causes of 20th-century channel narrowing in mountain and piedmont rivers of southeastern France. Earth Surf. Process. Landforms 27, 425–444.
Leontaritis, AD, Baltas, E, 2014. Hydrological Analysis of the Aoos (Vjosë) –Voidomatis Hydrosystem in Greece. Austin J Hydrol 1 (2), 8.
J.P. Martín-Vide, C. Ferrer-Boix, A. Ollero, Incision due to gravel mining: Modeling a case study from the Gállego River, Spain, Geomorphology, Volume 117, Issues 3–4, 2010, Pages 261-271, ISSN 0169-555X.
Milan, D.J., 2012. Geomorphic impact and system recovery following an extreme flood in an upland stream: Thinhope Burn, northern England, UK. Geomorphology 138 (1), 319–328.
Monegaglia, F., Zolezzi, G., Güneralp, I., Henshaw, A.J., Tubino, M., 2018. Automated extraction of meandering river morphodynamics from multitemporal remotely sensed data. Environ. Model. Software 105, 171–186.
Niroumand-Jadidi, M., Vitti, A., 2017. Reconstruction of river boundaries at sub-pixel resolution: estimation and spatial allocation of water fractions. ISPRS Int. J. Geo-Inf. 6 (12), 383.
Peters, R., Berlekamp, J., Lucía, A., Stefani, V., Tockner, K., Zarfl, C., 2021. Integrated impact assessment for sustainable hydropower planning in the Vjosa catchment (Greece, Albania). Sustainability 13, 1514.
Piégay, H., Arnaud, F., Belletti, B., Bertrand, M., Bizzi, S., Carbonneau, P., Dufour, S., Liébault, F., Ruiz-Villanueva, V., Slater, L., 2020. Remotely sensed rivers in the Anthropocene: state of the art and prospects. Earth Surf. Process. Landforms 45 (1), 157–188.
Rădoane, M., Obreja, F., Cristea, I., Mihailă, D., 2013. Changes in the channel-bed level of the eastern Carpathian rivers: climatic vs. human control over the last 50 years. Geomorphology 193, 91–111.
Rinaldi, M., Surian, N., Comiti, F., Bussettini, M., 2015. A methodological framework for hydromorphological assessment, analysis and monitoring (IDRAIM) aimed at promoting integrated river management. Geomorphology 251, 122–136.
Schiemer, F., Drescher, A., Hauer, C., Schwarz, U., 2018. The Vjosa River corridor: a riverine ecosystem of European significance. Acta ZooBot Austria 155, 1–40.
Schiemer, F., Beqiraj, S., Drescher, A., et al., 2020. The Vjosa River corridor: a model of natural hydro-morphodynamics and a hotspot of highly threatened ecosystems of European significance. Landsc. Ecol. 35 (4), 953–968.
Schmitt, R.J.P., Bizzi, S., Castelletti, A., Kondolf, G.M., 2018. Improved trade-offs of hydropower and sand connectivity by strategic dam planning in the Mekong. Nat. Sustain. 1 (2), 96–104.
Scorpio, V., Piégay, H., 2021. Is afforestation a driver of change in Italian rivers within the Anthropocene era? Catena 198, 105031.
Scorpio, V., Aucelli, P.P.C., Giano, S.I., Pisano, L., Robustelli, G., Rosskopf, C.M., Schiattarella, M., 2015. River channel adjustments in Southern Italy over the past 150 years and implications for channel recovery. Geomorphology 251, 77–90.
Shen, M., Liu, X., 2021. Assessing the effects of lateral hydrological connectivity alteration on freshwater ecosystems: a meta-analysis. Ecol. Indicat. 125, 107572.
Skoulikidis, N.T., Zogaris, S., Karaouzas, I., 2022. Rivers of the Balkans. Riv. Eur. 593–653.
Smirnov, H., 1939. Sur les Écarts de la Courbe de Distribution Empirique. Recueil Mathématique (Matematiceskii Sbornik) 6 (48), 3–26.
Spada, D., Molinari, P., Bertoldi, W., Vitti, A., Zolezzi, G., 2018. Multi-temporal image analysis for fluvial morphological characterization with application to Albanian rivers. ISPRS Int. J. Geo-Inf. 7 (8), 314.
Stecca G., Zolezzi G., Hicks D. Murray , Surian N., Reduced braiding of rivers in human-modified landscapes: Converging trajectories and diversity of causes, Earth-Science Reviews, Volume 188, 2019, Pages 291-311, ISSN 0012-8252.
Surian, N., 2022. Fluvial changes in the Anthropocene: a European perspective. In: Reference Module in Earth Systems and Environmental Sciences, Treatise on Geomorphology, second ed., pp. 561–583.
Surian, N., Rinaldi, M., 2003. Morphological response to river engineering and management in alluvial channels in Italy. Geomorphology 50 (4), 307–326.
Surian, N., Ziliani, L., Comiti, F., Lenzi, M.A., Mao, L., 2009. Channel adjustments and alteration of sediment fluxes in gravel-bed rivers of North-Eastern Italy: potentials and limitations for channel recovery. River Res. Appl. 25, 551–567.
Tickner, D., Opperman, J.J., Abell, R., Acreman, et al., 2020. Bending the curve of global freshwater biodiversity loss: an emergency recovery plan. Bioscience 70 (4), 330–342.
Tockner, K., Uehlinger, U., Robinson, C.T., Siber, R., Tonolla, D., Peter, F.D., 2009. European rivers. In: Likens, Gene E. (Ed.), Encyclopedia of Inland Waters, vol. 3. Elsevier, Oxford, pp. 366–377.
Tonolla, D., Geilhausen, M., Doering, M., 2021. Seven decades of hydrogeomorphological changes in a near-natural (Sense River) and a hydropower-regulated (Sarine River) pre-Alpine river floodplain in Western Switzerland. Earth Surf. Process. Landforms 46, 252–266.
Tunnicliffe, J., Brierley, G., Fuller, I.C., Leenman, A., Marden, M., Peacock, D., 2018. Reaction and relaxation in a coarse-grained fluvial system following catchment-wide disturbance. Geomorphology 307, 50–64.
Vercruysse, K., Grabowski, R.C., 2021. Human impact on river planform within the context of multi-timescale river channel dynamics in a Himalayan river system. Geomorphology 381, 107659.
Wagner, B., Hauer, C., Habersack, H., 2019. Current hydropower developments in Europe. Curr. Opin. Environ. Sustain. 37, 41–49.
Ward, J., Tockner, K., Edwards, P., Kollmann, J., Bretschko, G., Gurnell, A.M., Petts, G.E., Rossaro, B., 1999. A reference river system for the Alps: the 'Fiume Tagliamento'. Regulated rivers. Res. Manag. 15, 63–75.
Wohl, E., 2017. Connectivity in rivers. Prog. Phys. Geogr. 41 (3), 345–362.
Wohl, E., Bledsoe, B.P., Jacobson, R.B., Poff, N.L., Rathburn, S.L., Walters, D.M., Wilcox, A.C., 2015. The natural sediment regime in rivers: broadening the foundation for ecosystem management. Bioscience 65 (4), 358–371.
Xu, H., 2006. Modification of normalised difference water index (NDWI) to enhance open water features in remotely sensed imagery. Int. J. Rem. Sens. 27 (14), 3025–3033.
Young, M.A., Patel, K., Crenshaw, L.C., Moran, M.D., McClung, M.R., Chomphosy, W.H., 2022. Ecosystem services of the Buffalo national River in Arkansas. Nat. Area J. 42 (4), 293–300.
Zarfl, C., Lumsdon, A.E., Berlekamp, J., et al., 2015. A global boom in hydropower dam construction. Aquat. Sci. 77, 161–170.
Zarfl, C., Berlekamp, J., He, F., Jähnig, S.C., Darwall, W., Tockner, K., 2019. Future large hydropower dams impact global freshwater megafauna. Sci. Rep. 9 (1), 18531.
Zawiejska, J., Wyżga, B., 2010. Twentieth-century channel change on the Dunajec River, southern Poland: patterns, causes and controls. Geomorphology 117 (3–4), 234–246.
Ziliani, L., Surian, N., 2012. The evolutionary trajectory of channel morphology and controlling factors in a large gravel-bed river. Geomorphology 173–174, 104–117.
W. Bertoldi, N. A. Drake, A. M. GurnellHow to citeBertoldi, W., Drake, N.A. and Gurnell, A.M. (2011), Interactions between river flows and colonizing vegetation on a braided river: exploring spatial and temporal dynamics in riparian vegetation cover using satellite data. Earth Surf. Process. Landforms, 36: 1474-1486. https://doi.org/10.1002/esp.2166.